ISTANBUL TECHNICAL UNIVERSITY ★ INSTITUTE FOR NUCLEAR ENERGY

THERMAL-HYDRAULIC ANALYSIS OF I.T.U. TRIGA MARK-II REACTOR

M.Sc. THESIS

Emin Hakan ÖZKUL, B.Sc. Mech.Eng.

Date of Submission : 05 June 2000

Date of Defence Examination : 19 June 2000

Examination Committee

Supervisor (Chairman)	:	Assoc.Prof. Dr. Ahmet DURMAYAZ 30.06.2000
Member	:	Prof. Dr. Hasbi YAVUZ 29.06.2000
Member	:	Prof. Dr. Burhanettin CAN (MÜ) 20.07.2000

JUNE 2000

İSTANBUL TEKNİK ÜNİVERSİTESİ ★ NÜKLEER ENERJİ ENSTİTÜSÜ

İ.T.Ü. TRIGA MARK-II REAKTÖRÜNÜN TERMAL-HİDROLİK ANALİZİ

YÜKSEK LİSANS TEZİ

Mak. Müh. Emin Hakan ÖZKUL.

Tezin Enstitüye Verildiği Tarih : 05 Haziran 2000
Tezin Savunulduğu Tarih : 19 Haziran 2000

Tez Danışmanı : Doç. Dr. Ahmet DURMAYAZ
Diğer Jüri Üyeleri Prof. Dr. Hasbi YAVUZ
Prof. Dr. Burhanettin CAN (MÜ)

HAZİRAN 2000

PREFACE

In this study, a one-dimensional subchannel analysis has been carried out to investigate the transient thermal-hydraulic behaviour of I.T.U. TRIGA Mark-II reactor.

I would like to express my deepest gratitude to my supervisor, Associate Prof. Dr. Ahmet DURMAYAZ, for his perfect guidance and kind interest.

I would also like to thank the following professors for their valuable advice and support during the time I prepared and wrote my thesis: Prof. Dr. Hasbi YAVUZ, Prof. Dr. Burhanettin CAN, Associate Prof. Dr. Cihat BAYTAŞ and Prof. Dr. Melih GEÇKİNLİ.

I will also thank Assistant Prof. Dr. Tayfun BÜKE, since he helped me kindly to evaluate the results of my studies.

Finally, I sincerely thank my family for standing patiently behind my studies with continuous support for so many years.

CONTENTS

NOMENCLATURE

A	=	Area
a	=	General symbol for the coefficients
b	=	Source coefficient
c	=	Specific heat
D	=	Diameter
D	=	Diffusion strength
F	=	Convection strength, flow coefficient
F	=	Body force
g	=	Gravitational acceleration
h	=	Height
J	=	Total flux
k	=	Heat conductivity
P	=	Perimeter
P	=	Absolute pressure, total pressure
p	=	Pressure
q	=	Heat
q	=	Heat flux
q		Volumetric rate of heat generation
r	=	Radius; coordinate
Re	=	Reynolds number
S	=	Source term
T	=	Temperature
T	=	Time
v	=	Velocity
x, y, z	=	Coordinates
$[\![A,B,C,\ldots]\!]$	=	Largest of A, B, C, . . .

Subscripts

A	=	Atmospheric
$B,\ C,\ D,\ E$	=	Ring
c	=	Constant
cl	=	Clad
d	=	Dynamic
E	=	Neighbor in the positive z-direction
e	=	Control volume face between P and E
f	=	Fuel rod
fr	=	Friction

in	=	Inlet
m	=	Coolant
out	=	Outlet
p	=	At constant pressure
r, θ, z	=	Coordinates
surf	=	Surface
W	=	Neighbor in the negative z-direction
w	=	Control volume face between P and W
z-s , *x*	=	Cross-section perpendicular to the z-dimension
0	=	Reference point

Superscripts

0	=	Old value (at time t) of variable
*	=	Previous iteration value of a variable; also velocities based on a guessed pressure

Greek symbols

β	=	Thermal expansion coefficient
Δ	=	Difference
δ	=	Difference
Φ	=	General dependent variable; dissipation term
μ	=	Dynamic viscosity
ρ	=	Density

LIST OF TABLES

LIST OF FIGURES

ÖZET

Bu çalışmada, İ.T.Ü. TRIGA Mark-II Reaktörü'nün termal-hidrolik analizi kontrol hacmi yaklaşımı yöntemi kullanılarak bir boyutlu olarak yapılmıştır. Reaktör havuzunun içinde düşey konumda bulunan silindirik yakıt çubuklarının soğutulması, havuz içerisinde akışkanın ısınması sonucu oluşan yoğunluk farkına dayanan doğal konveksiyonla gerçekleştirilmektedir. Ancak, bu çalışmada reaktör içindeki akış modeli olarak en genel halde çözüm verebilecek bir model öngörülerek doğal ve zorlanmış taşınımın aynı anda dikkate alındığı birleşmiş taşınım esas alınmıştır. Soğutucu akışkana ait enerji korunumu ve momentum dengesi denklemlerinin çözümü eksenel doğrultuda yapılmıştır. Reaktör kalbinde düşey konumda birbirine paralel olarak bulunan yakıt çubukları, soğutucu akışkan için gözenekli bir yapı meydana getirirler. Bu yüzden akışkan akışının termal-hidrolik analizinin yapılması, bazı yaklaşımlar yapılmasını gerekli kılar. Bu çalışmada alt kanal analizi yöntemi kullanılarak, reaktör kalbi bölgesindeki akışkan akışı modellenmiştir. Reaktör kalbinin merkezi etrafında artarda dizili bulunan yakıt halkalarının düzgün geometrisi, bu çalışmada yakıt çubuğu merkezli alt kanal analizi yaklaşımında bulunulmasını sağlayan en önemli etken olmuştur. Bu sayede akış alanı, hidrolik çap, yakıt çubuklarının sürtünme yüzeyleri gibi termal-hidrolik analiz esnasında belirlenmesi gereken pek çok parametre kolayca tayin edilmiştir. Ayrıca, yakıt çubuğu halkalarının her konumunda basınç, hız gibi özeliklerin açısal doğrultuda değişmediği öngörüsü yapılmış ve böylece pek çok parametre kolayca belirlenmiştir. Soğutucu akışkanın modellenmesi, eksenel doğrultuda bir boyutlu olarak yapılmış, ayrıca seçilen alt kanallar arasında çapsal doğrultudaki kütle, momentum ve enerji geçişinin etkisi ihmal edilmiştir.

Soğutucu akışkana ait eksenel doğrultudaki enerji korunumu ve momentum dengesi denklemlerinin çözümlenmesi esnasında yakıt çubuklarından soğutma suyuna yapılan ısı transferi hesaplanarak dikkate alınmıştır. Yakıt çubuklarından soğutucu akışkana olan ısı transferinin hesaplanması ise bu yakıt çubuklarındaki hacimsel ısı kaynağı teriminin belirlenerek yakıt içerisinde radyal doğrultudaki ısı iletimi denkleminin çözümlenmesini gerektirir.

Bu çalışmada yukarıda özetle açıklanan nedenlerle, incelenen akışkan için enerji korunumu ve momentum dengesi denklemlerinin eksenel doğrultuda; ayrıca yakıt çubukları için ısı iletimi denkleminin çapsal doğrultuda integralleri alındıktan sonra kontrol hacmi varsayımı altında sonra ayrıklaştırılmaları yapılmıştır. Ayrıklaştırma işlemleri tamamlanarak elde edilen cebirsel denklem seti SIMPLE Algoritması'na göre çözümleme yapmak üzere geliştirilen bir FORTRAN programı vasıtası ile çözülmüştür. Böylece, hem daimi rejimde, hem de geçici rejimde yakıt çubuklarının ve soğutucu akışkanın sıcaklık dağılımı ve bunun yanı sıra soğutucu akışkana ait hız, basınç ve sıcaklık dağılımları elde edilmiştir.

SUMMARY

In this study, a transient, one-dimensional thermal-hydraulic analysis for ITU TRIGA Mark-II Reactor was achieved. The cooling principle of TRIGA Mark-II is based on natural convection. However, mixed convection has been considered for the modeling of this study in order to have a general usage purpose.

The parallel fuel rods in vertical position form a porous structure for the coolant fluid. The fluid, flowing among this porous media impels us to apply an approach so as to achieve the thermal-hydraulic analysis. We have employed a subchannel analysis in this study because the regular geometry of the fuel rings provides us simplicity during the application. By this way, several parameters of the fluid (i.e. flow area, hydraulic diameter, power density, etc.) can easily be determined and used safely during the thermal-hydraulic analysis.

After the integration of the governing equations, the one dimensional conservation of energy equation, momentum balance equation in axial direction, and one dimensional heat conduction equation in radial direction have been discretized. by using the control volume approach to obtain a set of algebraic governing equations. Then, a pressure correction equation has been derived by the aid of the discretized continuity and momentum balance equations. Finally a FORTRAN programme has been developed to solve this set of algebraic equations by using SIMPLE algorithm. Hence, the temperature distribution of the cooling fluid and fuel rods have been determined. Additionally, the velocity and pressure distribution of the coolant has been designated.

CHAPTER 1

INTRODUCTION

1.1 I.T.U. TRIGA Mark-II Reactor

The I.T.U. TRIGA (Training Research Isotop Production General Atomics) Mark-II reactor was designed to fulfil the need for a safe research reactor that combines unique radioisotope-producing capabilities with experimental and training facilities. The reactor is operated in two different modes: steady state and pulsing. Reactor power levels in the steady-state mode ranges up to and includes 250 kW. Pulse mode operation takes place by step reactivity insertions with the reactor initially at a power less than 1 kW. The maximum step reactivity insertion is 2.1% $\delta k/k$ ($3.00) which produces a peak reactor power of approximately 1200 MW(th) for a few ten milliseconds [1,2].

The reactor core shown in Fig. 1.1 is located at the bottom of an aluminum tank in the center of a concrete shield structure called biological shield. The aluminium tank is pierced by the beam tubes and the thermal column for irradiation purposes.

The primary cooling system seen in Fig.1.2 consists of a pump, a heat exchanger, temperature probes, an N-16 diffuser, associated valves and piping. The primary cooling system pump is a centrifugal type.

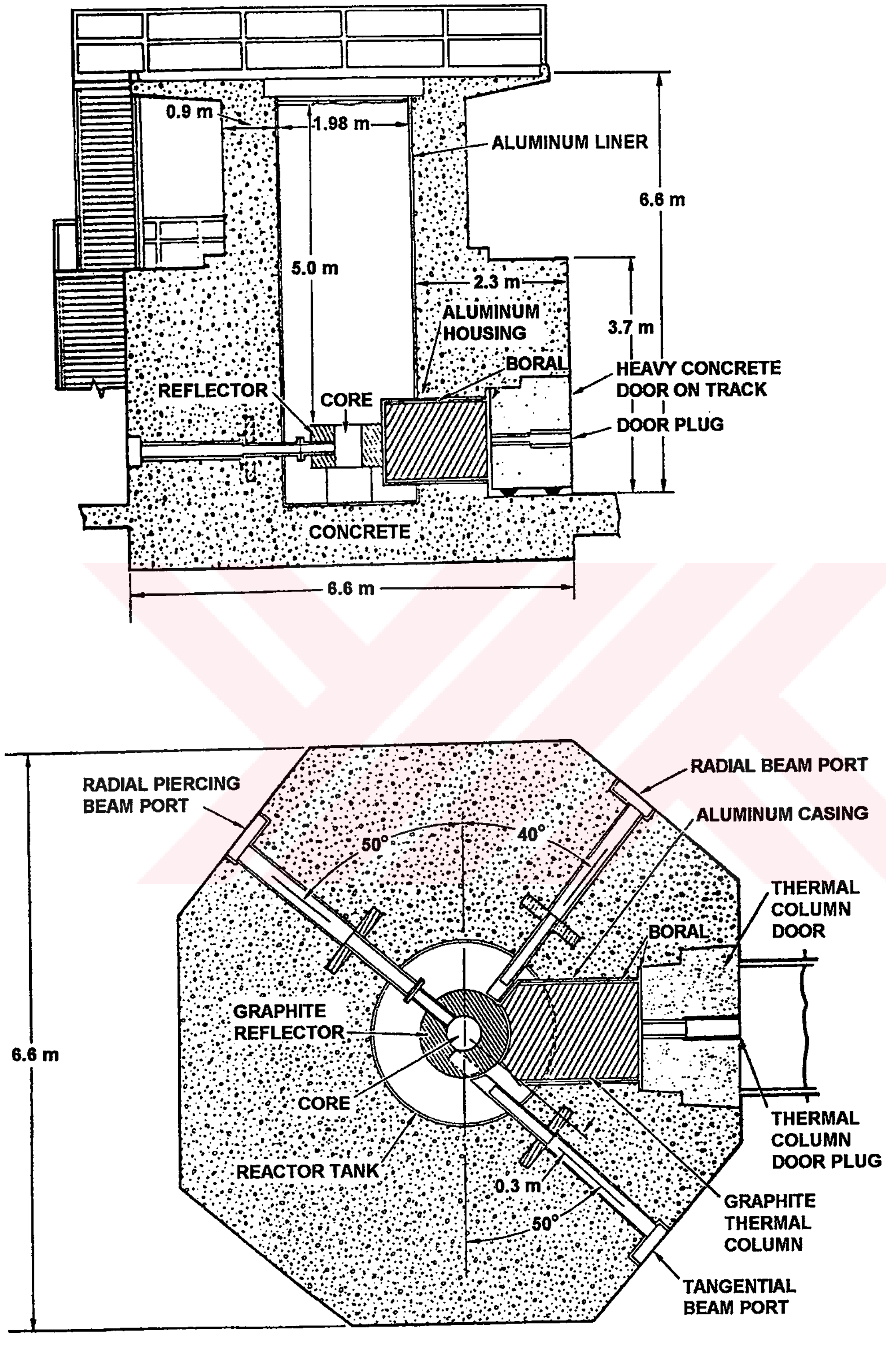

Figure 1.1. Cutaway View of I.T.U. TRIGA Mark-II Reactor [1,2]

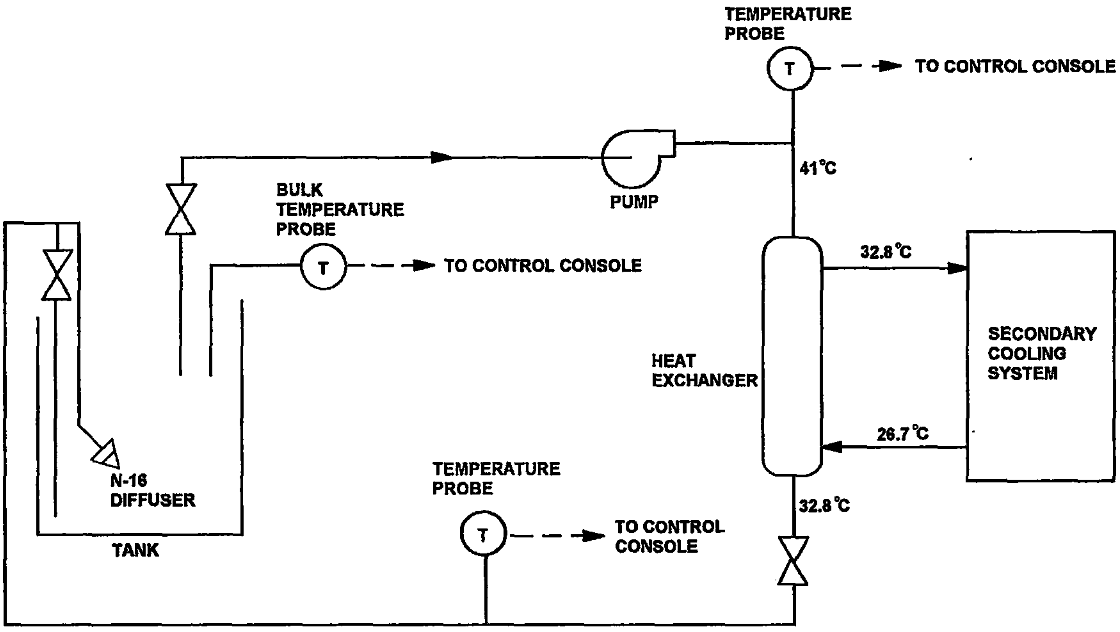

Figure 1.2 Primary Cooling Loop of TRIGA Mark-II Reactor [1,2]

The core consists of ninety vertical cylindrical elements located in five rings around the central thimble, shown in Fig.1.3. Sixty-nine of them are fuel elements. The structure of a fuel element is shown in Fig.1.4. These fuel elements consists of four components:

1- fuel moderator meat

2- graphite reflectors

3- cladding

4- end fixtures

The fuel meat section is homogenous mixture of zirconium and uranium. The uranium content of this mixture is 8.5% by weight with an enrichment of 20% of U^{235}. This mixture is processed and finally extruded to a diameter of 3.63 cm and cut into 3 fuel meats having a total length of

38.1 cm. Each fuel meat is then subjected to a sensitive hydriding process (that depends upon time, temperature and pressure) to provide a hydrogen-

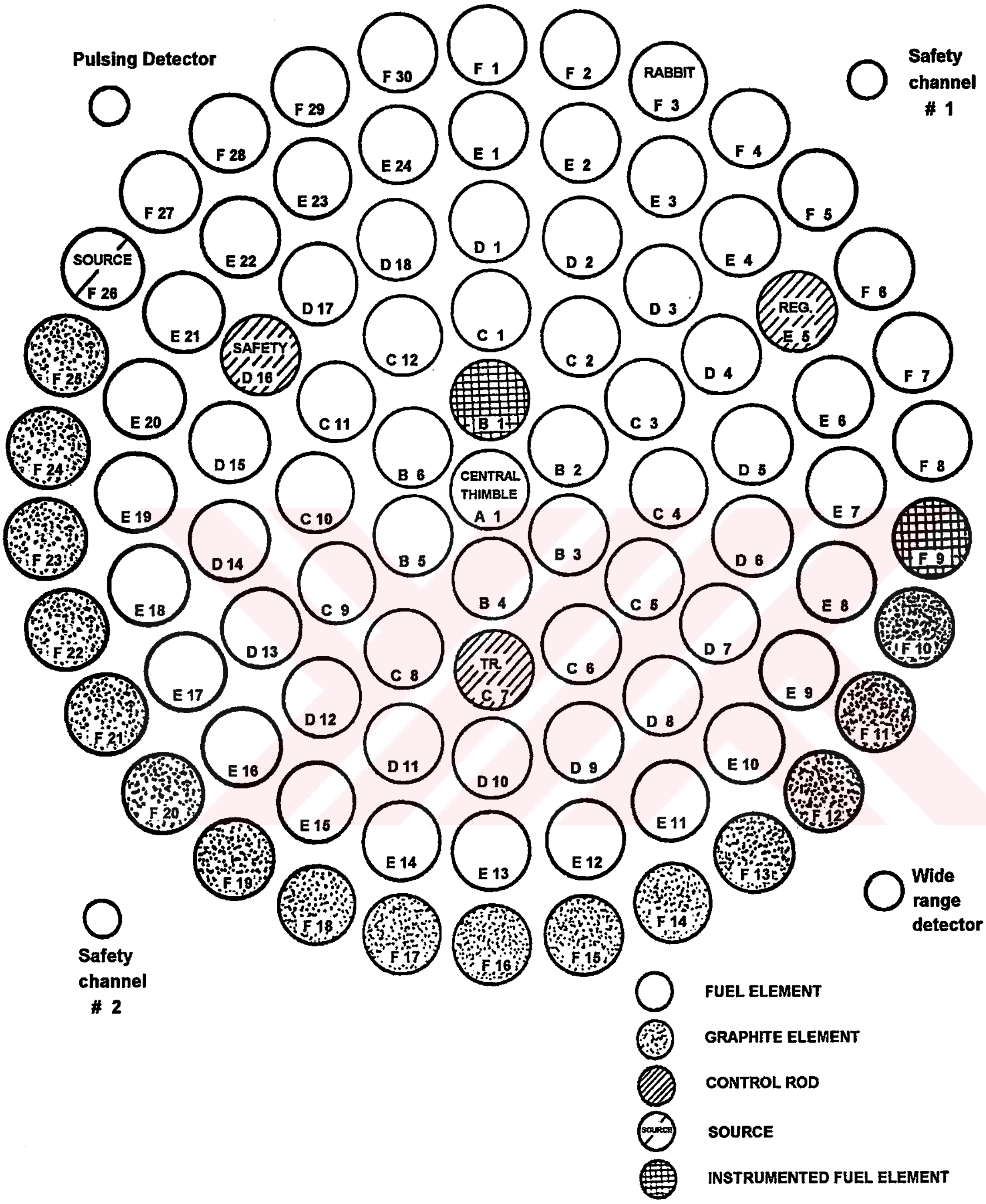

Figure 1.3. ITU TRIGA Mark-II Reactor Core Diagram [1,2]

to-zirconium atom ratio of H/Zr = 1.7. To facilitate a uniform hydriding, a hole (0.06 cm) is drilled axially along the centre of the fuel meat. Upon completion of hydriding, a zirconium rod is inserted into this hole. Each

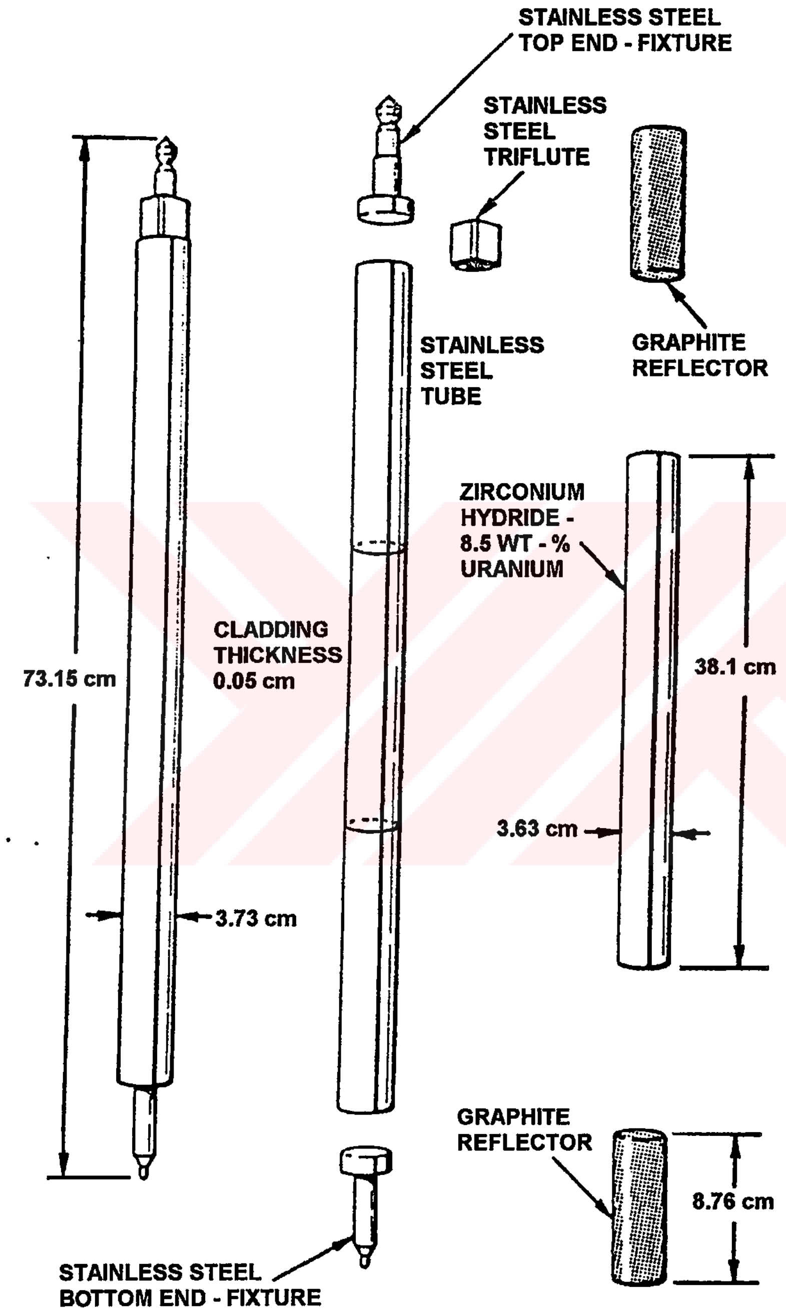

Figure 1.4 Typical TRIGA stainless-steel-clad fuel element [1,2]

fuel element contains two graphite reflectors 8.76 cm long, one at each end of the fuel meat. These graphite reflectors serve as a top and bottom reflector for the core. The fuel-moderator meat and graphite reflectors are housed in a stainless steel cladding can which has a wall thickness of 0.05 cm. The top and bottom end fixtures are the plugs for the cladding can and accordingly are welded in place. The main function of these end fixtures is to fix the fuel elements to the grid plates.

TRIGA fuel elements are spaced and supported in the core by means of aluminium top and bottom grid plates similar to those shown in Figs. 1.5. and 1.6 The bottom grid plate is approximately 0.3 cm thick with spaces to permit coolant passage through the plate and to receive the fuel element lower end fixtures. The upper grid plate provides lateral support for the fuel elements, but the entire weight of the fuel elements rests on the lower grid plate. Holes approximately 0.2-0.4 cm in diameter have been drilled in the 0.3-cm thick top grid plate to space the fuel elements and allow their withdrawal from the core.

The safety analysis of TRIGA Mark–II reactor requires the determination of the fuel temperature not only in steady state mode, but also in transient regime. Since increase in temperature depends on the flow model of the coolant, such a safety analysis can only be obtained by a thermal-hydraulic model of the reactor core.

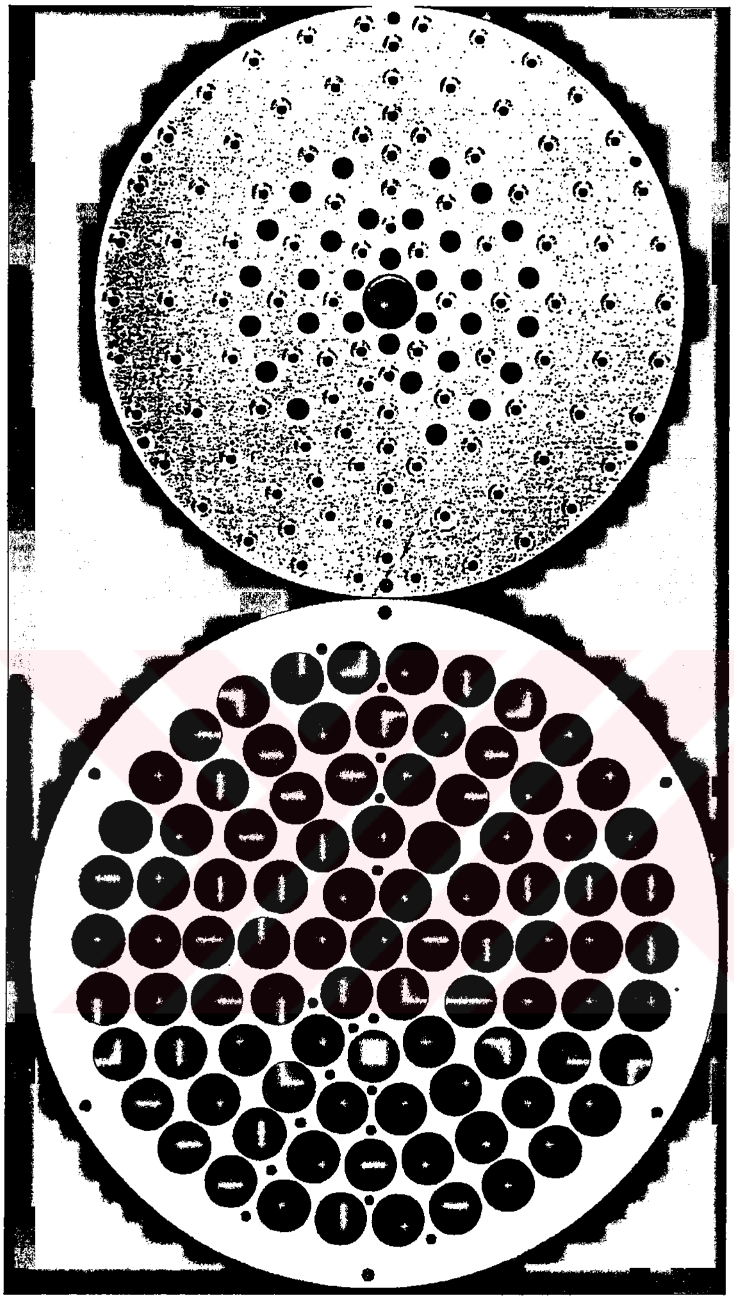

Fig. 1.5 Top and bottom grid plates [2]

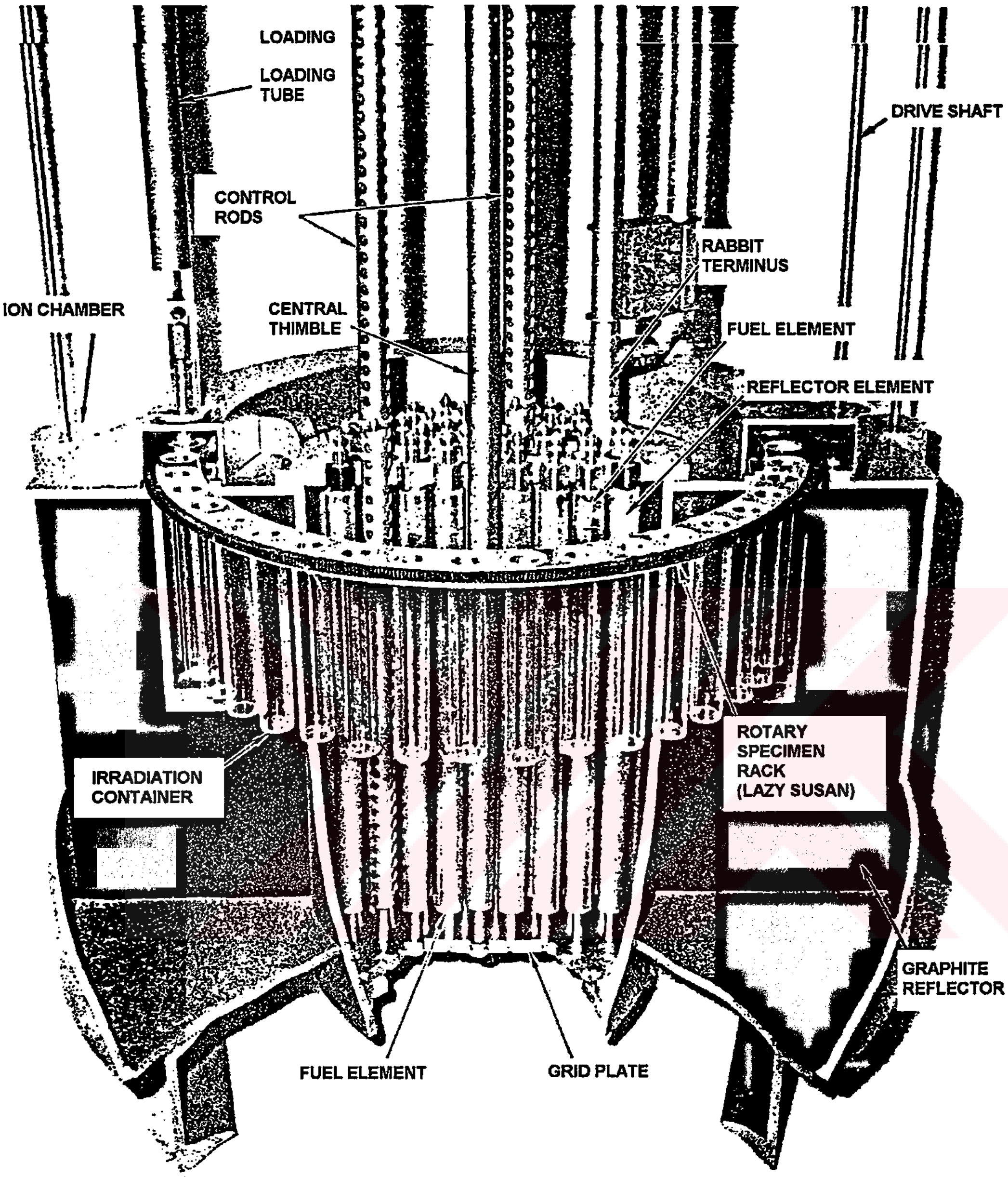

Figure 1.6 Cutaway model of typical reflector [2]

1.2 The Thermal-Hydraulic Model

Reactor cooling is provided by natural circulation of pool water, which is in turn cooled and purified in external coolant circuits by forced convection. Therefore, this characteristic cooling system of the tank water basing on both natural and forced convection drives us to consider mixed convection for the determination of the flow model in general.

In this study, a subchannel analysis was preferred for the thermal-hydraulic model of I.T.U. TRIGA Mark-II reactor. Some different analysing methods could also have been taken up instead. In fact, "**the porous media approach**" is a practical method for the thermal hydraulic analysis of reactor cores, and is widely used in nuclear engineering. However, the employment of this approach depends on the value of porosity of the surfaces. Since the value of porosity is too small in the I.T.U. TRIGA Mark-II reactor core, this drives us to choose a "**subchannel analysis**" model, in which subchannel properties like axial directional velocity and density are represented by single area averaged values. Constitutive relations are required as the input parameters like friction factors and lateral momentum and energy exchange rates between adjacent subchannels, if they are considered. This choice of nodal layout in terms of subchannels does not yield simpler constitutive equations than would other choices. Rather, it offers a convenient arrangement for which a specific set of constitutive equations can be formulated. In a practical sense, this leads to a focussing of effort on a single set of constitutive relations [3-8].

Further, in the subchannel approach a major simplification is the treatment of lateral exchanges between adjacent subchannels. A fully three dimensional physical solution can be represented simply by connecting the channels in a three-dimensional array. This leads to simplifications in the lateral convective terms of the linear momentum balance equation that makes the method most appropriate for predominantly axial flow situations. The subchannel analysis approach and its associated boundary conditions are therefore not a fully three-dimensional representation of the flow.

The subchannel analysis method contains two different types of approaches: the coolant centred and the rod centred subchannels as illustrated in Fig. 1.7. The traditional approach for rod bundle analysis has been coolant-centred subchannels.

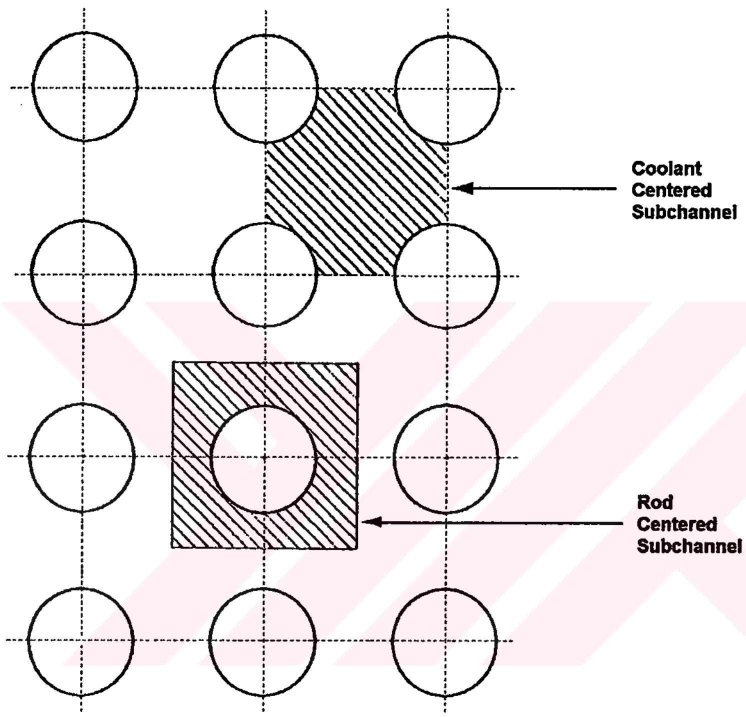

Figure 1.7 Options for subchannel definition [9]

A typical control volume chosen in the axial direction in a coolant centred subchannel is shown in Fig.1.8.

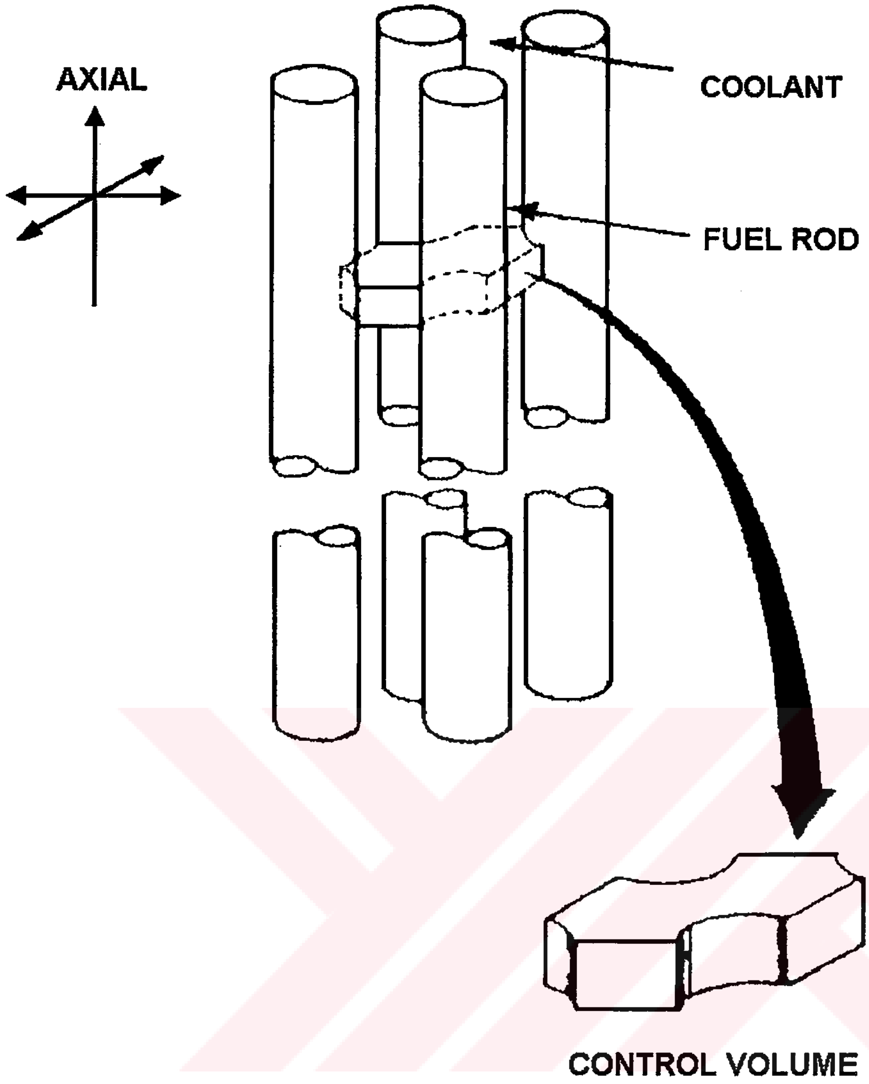

Figure 1.8 A typical control volume in a coolant centred subchannel [9]

Since the rod-centred subchannel approach provides us a regular, well-arranged geometry, it has been taken up in this study as shown in Fig. 1.9.

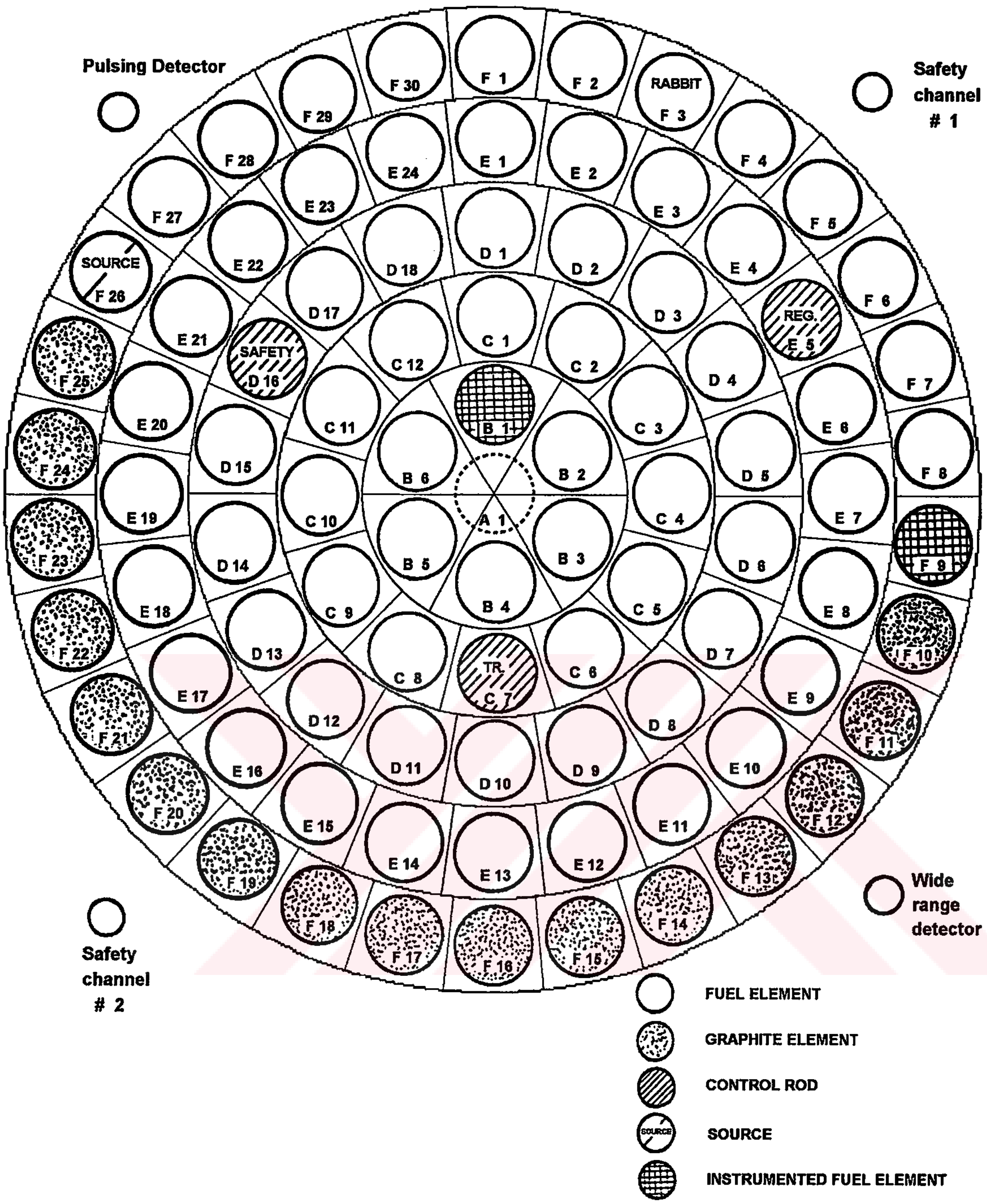

Figure 1.9. Selection of the subchannels on ITU TRIGA Mark-II Reactor Core

Therefore, the thermal-hydraulic parameters can easily be calculated for the rod centred subchannels. In ITU TRIGA Mark-II reactor core, we shall call each subchannel by the same name of its rod it contains. For instance, the subchannel C_1 is the one around the rod C_1.

Let us, as an example, calculate some parameters for a subchannel that take place in ring C by the aid of Fig. 1.10.

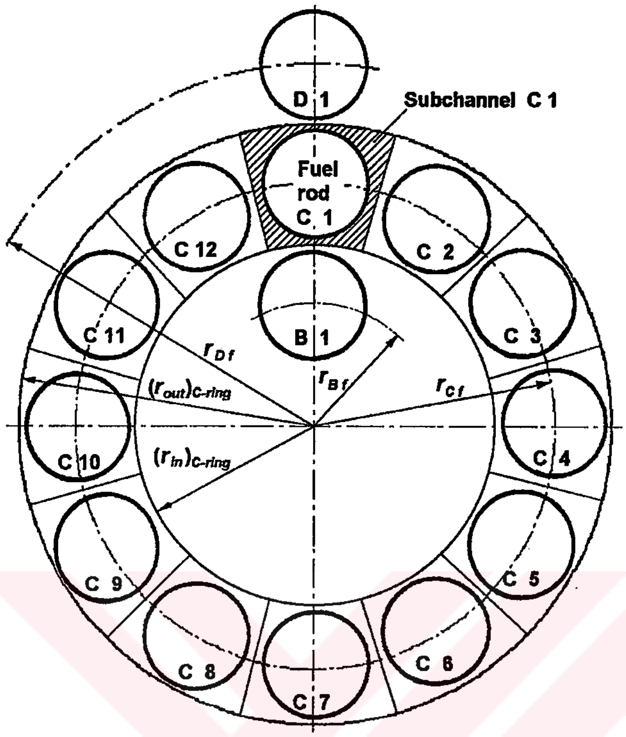

Figure 1.10. Ring C and the subchannel C1 on ITU TRIGA Mark-II Reactor Core

The area of ring C is

$$A_{C-ring} = \pi\left(r_{out}^2 - r_{in}^2\right)_{C-ring} \tag{1.1}$$

where

$$\left(r_{in}\right)_{C-ring} = \frac{\left(r_{Bf} + r_{Cf}\right)}{2} \tag{1.2}$$

and

$$\left(r_{out}\right)_{C-ring} = \frac{\left(r_{Cf} + r_{Df}\right)}{2} \tag{1.3}$$

while r_{Bf}, r_{Cf} and r_{Df} are the distances from the reactor core of the centre of the rods that take place in rings B, C and D respectively.

Since there are 12 rods in the C ring, the flow area of a subchannel in Ring C can be written as:

$$A_{C_i} = \frac{\left(A_{C-ring} - 12\pi r_{fuel}^2\right)}{12} \quad , \; i = 1,12 \qquad (1.4)$$

The hydraulic diameter of a subchannel is the equivalent diameter for the considered cross-sectional area of the fluid in the subchannel. Hydraulic diameter is used for the calculation of Reynolds number in this thermal-hydraulic model.

The area for the frictional force in a subchannel is equal to the outer surface area of the rod, which is

$$A_{fr} = 2\pi r_{rod} h_{rod} \qquad (1.5)$$

where r_{rod} and h_{rod} are the radius of the rod and the height of the active fuel meat respectively.

According to our model, calculated flow area, hydraulic diameter and frictional area for each ring of I.T.U. TRIGA Mark-II reactor core can be summarised as seen in Table 1.1.

The frictional area values in in Table 1.1 express the frictional area in the in the subchannels among the fuel meats. Thus we used the value of $h_{rod} = 38.1 cm$ for the calculation of these frictional areas. If the height of a control volume were employed, the frictional area in that control volume would be obtained.

Table 1.1 Some parameters of I.T.U. TRIGA Mark-II reactor core according to the thermal-hydraulic model considered by this study.

Subchannels in the rings:	Distance from the core centre, R_f (cm)	Flow area (cm^2)	Hydraulic diameter (cm)	Frictional area (cm^2)
B	4.054	5.859	2.731	446.916
C	7.981	5.560	2.661	446.916
D	11.946	5.461	2.637	446.916
E	15.860	5.564	2.662	446.916

1.2.1 Assumptions and Correlations used in the Thermal-Hydraulic Model

We apply the following assumptions in our thermal-hydraulic model:

1- There is no mass, momentum or energy transfer between the subchannels in r- and θ-directions.

2- Since almost all of the heat produced in the fuel is transferred to the coolant in radial direction, we neglect the heat transfer from the fuel to the top and bottom graphite reflectors in z-direction.

3- The thermal-hydraulic properties of the coolant are assumed to be equal in r- and θ-directions in any subchannel since we use area-averaged properties perpendicular to z-direction.

4- It is assumed that energy is produced homogeneously on the horizontal cross-section of a fuel.

5- The reactor works either in transient or steady state mode.

6- The core inlet temperature and velocity do not change in time.

7- The density ρ, dynamic viscosity μ, specific heat c_p and conductivity k of the coolant are functions of temperature and pressure. In this study, they have been calculated by means of the **H2O** computer program [3].

Nevertheless, the following correlations as functions of temperature for these expressions could also have been employed [4]:

$$\rho_m = 1.0017773 - 0.928*10^{-4}*T_m - 3.601*10^{-6}*T_m^2 ,$$
$$\text{for } 20 \le T_m \le 70^\circ\text{C}, \ 165 \text{ kPa} \qquad (1.6)$$

$$c_m = 4.18989 - 0.6371*10^{-3}*T_m + 9.22*10^{-6}*T_m^2 \qquad (1.7)$$

$$\mu_m = 1.4351*10^{-2} - 0.259*10^{-3}*T_m + 1.62*10^{-6}*T_m^2 \qquad (1.8)$$

$$k_m = 5.802*10^{-3} + 1.175*10^{-5}*T_m \qquad (1.9)$$

The Prandtl number has also been calculated in **H2O** computer program. Alternatively, the following correlation could have been employed [4]:

$$\Pr = 11.7261 - 0.3072*T_m + 3.786*10^{-3}*T_m^2 - 1.812*10^{-5}*T_m^3 \qquad (1.10)$$

The free convection heat transfer coefficient h_m on a vertical cylinder is obtained in terms of the dimensionless groups from the literature in the following functional forms [5]:

a) Laminar flow

$$h_m = 0.59\, k_m (Gr \Pr)_m^{0.25} / H \qquad 10^4 \le Gr \Pr \le 10^9 \qquad (1.11)$$

b) Turbulent flow

$$h_m = 0.10 (Gr \Pr)_m^{1/3} / H \qquad 10^9 \le Gr \Pr \le 10^{13} \qquad (1.12)$$

where the Grashoff number is

$$Gr = \frac{g \beta_m \rho_m^2}{\mu_m^2} (T_w - T_m) H^3 . \qquad (1.13)$$

8- It is assumed that the thermal conductivity and the specific heat of the fuel and the thermal conductivity of the clad are temperature-dependent. They have been calculated from the following equations [5]:

$$k_f = \frac{0.17585}{1 - 4.15 * 10^{-4} * T_f} \qquad (W/m-K) \qquad (1.14)$$

$$k_{cl} = \frac{13.4634}{1 - 9.6884 * 10^{-4} * T_{cl}} \qquad (W/m-K) \qquad (1.15)$$

$$c_f = 857 + 1.6(T_f - 25) \qquad (kj/kg-K) \qquad (1.16)$$

For the other physical properties of fuel and clad, the following constant values were employed:

$$c_{cl} = \ 460 \quad kj/kg-K \qquad (1.17)$$

$$\rho_f = 6000 \quad kg/m^3 \qquad (1.18)$$

$$\rho_{cl} = 7865 \ kg/m^3 \qquad (1.19)$$

CHAPTER 2

AREA AVERAGED CONSERVATION EQUATIONS

2.1 Basic Definitions

Some of the basic definitions, which will be used in the conservation equations, are given below [11].

The cross-sectional area average of an arbitrary variable ϕ is defined by the following symbol;

$$<\phi> \overset{\Delta}{=} \frac{1}{A_{x\text{-}s}} \iint_{A_{x\text{-}s}} \phi \, dA \tag{2.1}$$

In the thermal-hydraulic model we considered, all of the dependent variables become area averaged when the derivation of the formulation set is completed. However, we will denote any variable without using an area average symbol for simplicity.

2.2 Governing Equations

Three-dimensional continuity, momentum balance and conservation of energy equations in cylindrical coordinates for the coolant can be written as follows [12-16]:

2.2.1 Three-dimensional Continuity Equation

Three-dimensional continuity equation in cylindrical coordinates is

$$\frac{\partial \rho}{\partial t} + \frac{\partial(\rho v_r)}{\partial r} + \frac{\rho v_r}{r} + \frac{1}{r}\frac{\partial(\rho v_\theta)}{\partial \theta} + \frac{\partial(\rho v_z)}{\partial z} = 0 \tag{2.4}$$

where ρ is the density; v_r, v_θ and v_z are the r, θ and z directional velocity components of the coolant.

2.2.2 Three-dimensional Conservation of Energy Equation

Three-dimensional conservation of energy equation in cylindrical coordinates can be written as

$$\frac{\partial(\rho c_p T)}{\partial t}+\frac{\partial(\rho c_p v_r T)}{\partial r}+\frac{1}{r}\frac{\partial(\rho c_p v_\theta T)}{\partial \theta}+\frac{\partial(\rho c_p v_z T)}{\partial z}$$

$$=k\left[\frac{1}{r}\frac{\partial}{\partial r}\left(r\frac{\partial T}{\partial r}\right)+\frac{1}{r^2}\left(\frac{\partial^2 T}{\partial \theta^2}\right)+\frac{\partial^2 T}{\partial z^2}\right]+q'''+\Phi \tag{2.5}$$

where q''' is the volumetric heat strength; T, k and c_p are the temperature, of the coolant, conductivity and specific heat at constant pressure; Φ is the dissipation term.

2.2.3 Three-dimensional Momentum Balance Equations

Three-dimensional momentum balance equations in z, r and θ directions are as follows:

In z-direction:

$$\frac{\partial(\rho v_z)}{\partial t}+\frac{\partial(\rho v_r v_z)}{\partial r}+\frac{1}{r}\frac{\partial(\rho v_\theta v_z)}{\partial \theta}+\frac{\partial(\rho v_z v_z)}{\partial z}$$

$$=-\frac{\partial P}{\partial z}+\mu\left(\frac{\partial^2 v_z}{\partial r^2}+\frac{1}{r}\frac{\partial v_z}{\partial r}+\frac{1}{r^2}\frac{\partial^2 v_z}{\partial \theta^2}+\frac{\partial^2 v_z}{\partial z^2}\right)-F_z \tag{2.6}$$

In θ-direction:

$$\frac{\partial(\rho v_\theta)}{\partial t}+\frac{\partial(\rho v_r v_\theta)}{\partial r}+\frac{1}{r}\frac{\partial(\rho v_\theta v_\theta)}{\partial \theta}+\frac{v_r v_\theta}{r}+\frac{\partial(\rho v_z v_\theta)}{\partial z}$$

$$=-\frac{1}{r}\frac{\partial P}{\partial \theta}+\mu\left(\frac{\partial^2 v_\theta}{\partial r^2}+\frac{1}{r}\frac{\partial v_\theta}{\partial r}-\frac{v_\theta}{r^2}+\frac{1}{r^2}\frac{\partial^2 v_\theta}{\partial \theta^2}+\frac{2}{r^2}\frac{\partial v_r}{\partial \theta}+\frac{\partial^2 v_\theta}{\partial z^2}\right)-F_\theta \tag{2.7}$$

In r-direction:

$$\frac{\partial(\rho v_r)}{\partial t}+\frac{\partial(\rho v_r v_r)}{\partial r}+\frac{1}{r}\frac{\partial(\rho v_\theta v_r)}{\partial \theta}-\frac{{v_\theta}^2}{r}+\frac{\partial(\rho v_z v_r)}{\partial z}$$

$$=-\frac{\partial P}{\partial r}+\mu\left(\frac{\partial^2 v_r}{\partial r^2}+\frac{1}{r}\frac{\partial v_r}{\partial r}-\frac{v_r}{r^2}+\frac{1}{r^2}\frac{\partial^2 v_r}{\partial \theta^2}-\frac{2}{r^2}\frac{\partial v_\theta}{\partial \theta}+\frac{\partial^2 v_r}{\partial z^2}\right)-F_r \tag{2.8}$$

where P and μ are the absolute pressure and dynamic viscosity of the coolant; F_z, F_θ and F_r are the body force components in z, θ and r directions respectively.

In this study, our aim is to constitute a one-dimensional thermal-hydraulic model for simplicity .Therefore, we assume that the distribution of temperature, velocity and other dependent variables of coolant are uniform in the subchannels in θ and r directions. Thus, after integrating the three-dimensional equations over the cross-sectional flow area perpendicular to the z- (flow) direction, we can write the one-dimensional continuity, momentum balance and conservation of energy equations in cylindrical coordinates as follows:

2.2.4 One-dimensional Continuity Equation

Neglecting the area averaged operators, one-dimensional continuity equation in cylindrical coordinates can be written as

$$\frac{\partial \rho}{\partial t} + \frac{\partial(\rho v_z)}{\partial z} = 0 \tag{2.9}$$

2.2.5 One-dimensional Conservation of Energy Equation

If we neglect the effect of dissipation in Eq. (2.5) and divide all terms in this equation by c_p, we obtain the one-dimensional conservation of energy equation in z-direction in cylindrical coordinates as

$$\frac{\partial(\rho T)}{\partial t} + \frac{\partial(\rho v_z T)}{\partial z} = \frac{k}{c_p}\left(\frac{\partial^2 T}{\partial z^2}\right) + \frac{q'''}{c_p} \tag{2.10}$$

2.2.6 One-dimensional Momentum Balance Equation

In the following derivation for momentum equations, we shall derive only the z-directional momentum equation. The general form of the momentum balance equation is the equation for mixed convection. Using such kind of an equation, one can solve both forced convection and natural convection problems. Therefore, we shall add the buoyancy force term to this equation, since we consider that our z-direction is vertical.

In Eq. (2.6), the pressure term P expresses the absolute pressure. Absolute pressure is sum of the atmospheric pressure p_a, the dynamic pressure p_d and the hydraustatic pressure $\rho_0 gz$:

$$P = p_a + p_d + \rho_0 gz \tag{2.11}$$

After integrating Eq. (2.6) over the cross-sectional flow area perpendicular to the z-direction and substituting the pressure term given in Eq. (2.11), one can obtain

$$\frac{\partial(\rho v_z)}{\partial t} + \frac{\partial(\rho v_z v_z)}{\partial z} = -\frac{\partial}{\partial z}(p_a + p_d + \rho_0 gz) + \mu\left(\frac{\partial^2 v_z}{\partial z^2}\right) - \frac{\tau \mathrm{P}}{A_x} - \rho g \tag{2.12}$$

where $F_z = \rho g$ and g is the gravitational acceleration.

In Eq. (2.12), ρ is the density of the fluid and ρ_0 is the density of the region in the fluid where the temperature is T_0. Since the change in atmospheric pressure is zero, Eq. (2.12) can be written as

$$\frac{\partial(\rho v_z)}{\partial t} + \frac{\partial(\rho v_z v_z)}{\partial z} = -\frac{\partial p_d}{\partial z} + \mu\left(\frac{\partial^2 v_z}{\partial z^2}\right) - \frac{\tau \mathrm{P}}{A_x} - g(\rho_0 - \rho) \tag{2.13}$$

In Eq. (2.13), we assume that the density ρ in the last term is variable, while the density expressions at the other terms are constant. This assumption is known as ***Boussinesq Approach***.

The temperature dependent variation of fluid density under constant pressure is expressed by thermal expansion coefficient, β.

$$\beta = -\left(\frac{1}{\rho}\frac{\partial \rho}{\partial T}\right)_p \cong -\frac{1}{\rho}\left(\frac{\rho_0 - \rho}{T_0 - T}\right) \tag{2.14}$$

Using this definition,

$$\rho_0 - \rho = \rho\beta(T - T_0) \tag{2.15}$$

is obtained. By the aid of Eq. (2.15), Eq. (2.13) can also be written as

$$\frac{\partial(\rho v_z)}{\partial t}+\frac{\partial(\rho v_z v_z)}{\partial z}=-\frac{\partial p_d}{\partial z}+\mu\left(\frac{\partial^2 v_z}{\partial z^2}\right)-\frac{\tau \mathrm{P}}{A_x}-\rho g\beta(T-T_0) \tag{2.16}$$

Eq. (2.16) is the general form of the one-dimensional momentum equation written in z-direction in cylindrical coordinates for mixed convection.

CHAPTER 3

NUMERICAL SOLUTION PROCEDURE

3.1 Grid Structure

In this section, we will derive a set of algebraic equations from the differential equations given by Eqs. (2.9), (2.10) and (2.16) with the help of a staggered grid control volume approach. Grid for continuity, energy balance, and pressure correction equations is shown in Fig. 3.1a and staggered grid for momentum balance equation is shown in Fig. 3.1b [2].

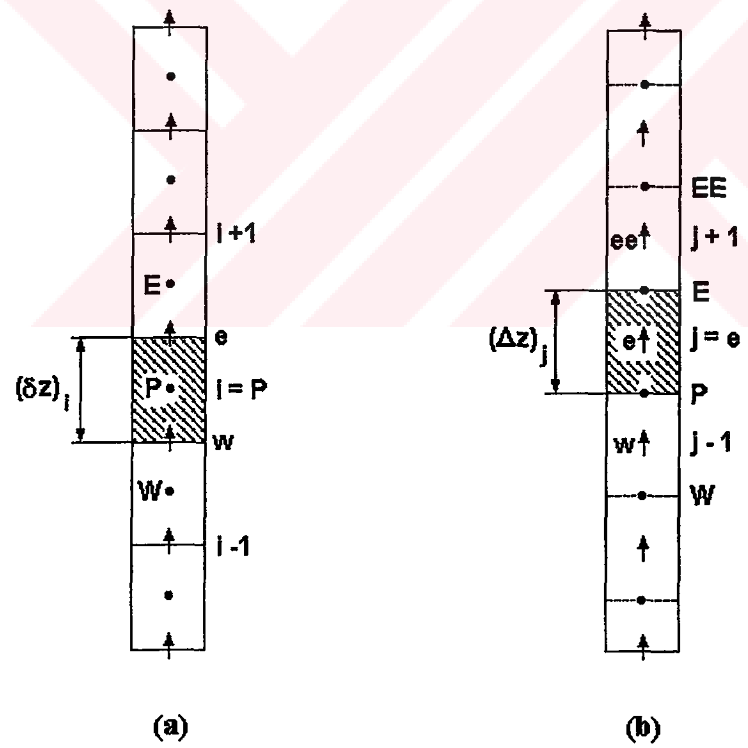

Figure 3.1 Grid (a) for continuity, energy balance, pressure correction equations and staggered grid (b) for momentum balance equation

3.2 Discretization Equations for the Conservation of Energy Equation

In this section, we will construct a numerical method for solving the conservation of energy equation, i.e. Eq. (2.10), [17,18].

We can indicate the source term of the conservation of energy equation simply as

$$S^T = \frac{q'''}{c_p} \tag{3.1}$$

S^T can be a constant or any function of temperature. When the source S depends on temperature, we express the linear dependence in a linear form given by Eq. (3.2).

$$S^T = S_c^T + S_P^T T_p \tag{3.2}$$

where S_c^T stands for the constant part of source term, while S_P^T is the coefficient of temperature, T_P.

Substituting this expression into Eq. (2.10), we obtain

$$\frac{\partial(\rho T)}{\partial t} + \frac{\partial(\rho v_z T)}{\partial z} = \frac{k}{c_p}\left[\frac{\partial^2 T}{\partial z^2}\right] + S_c^T + S_P^T T_p \tag{3.3}$$

It is useful to define a total flux J that is made up of the convective flux term ρuT and the diffusion flux term $(k/c_p)\frac{\partial T}{\partial z}$.

$$J^T = \rho v_z T A_x - \frac{k}{c_p}\frac{\partial T}{\partial z} A_x \tag{3.4}$$

Using this definition, if we integrate Eq. (3.3) over the control volume shown in Fig. 3.1a, we can write

$$\frac{(\rho T - \rho^0 T^0)_P}{\Delta t}(\Delta z A_x)_P + J_e^{\ T} - J_w^{\ T}$$

$$= \left(S_c^T\right)_P (\Delta z)_P (A_x)_P + \left(S_P^T\right)_P T_P (\Delta z)_P (A_x)_P \tag{3.5}$$

In this integration process, we use fully implicit scheme, so that the values of temperature and density at time $t+\Delta t$ are assumed to prevail over the entire time step; the old density ρ_P^0 and the old temperature T_P^0 (i.e., the ones at time t) appears only in the first term of Eq. (3.5).

If we also integrate the continuity equation, i.e., Eq. (2.9) over the same control volume in conformity with the implicit scheme, we obtain

$$\frac{\left(\rho-\rho^0\right)_P}{\Delta t}(\Delta z A_x)_P + \left(\rho v_z A_x\right)_e - \left(\rho v_z A_x\right)_w = 0 \tag{3.6}$$

If we multiply the terms of Eq. (3.6) by T_P, then subtract them from Eq. (3.5), we obtain

$$\frac{\rho_P^0 (\Delta z)_P (A_x)_P}{\Delta t}\left(T-T^0\right)_P + \left[J_e^T - \left(\rho v_z A_x\right)_e T_P\right] - \left[J_w^T - \left(\rho v_z A_x\right)_w T_P\right] =$$

$$\left(S_c^T\right)_P (\Delta z)_P (A_x)_P + \left(S_P^T\right)_P T_P (\Delta z)_P (A_x)_P \tag{3.7}$$

where the explicit form of the total flux term at the e-interface is

$$J^T{}_e = \left(\rho v_z A_x\right)_e T_e - \left(\frac{k}{c_p} A_x\right)_e \left(\frac{dT}{dz}\right)_e \tag{3.8}$$

We can indicate the temperature gradient simply as in the form given below:

$$J^T{}_e = \left(\rho v_z A_x\right)_e T_e - \left(\frac{k}{c_p \Delta z} A_x\right)_e (T_E - T_P) \tag{3.9}$$

To arrange the equation more compactly, we define two new symbols F^T and D^T, as follows:

$$F^T = \rho u Ax\ , \quad D^T = \frac{k A_x}{c_p \Delta z} \tag{3.10}$$

Both of these terms have the same dimensions; F^T indicates the strength of the convection (or flow), while D^T is the diffusion conductance. Now we can rewrite the total flux term as

$$J_e^T = F_e^T T_e - D_e^T (T_E - T_P) \tag{3.11}$$

Using similar derivations, the total flux at the w-interface can be written as

$$J_w^T = F_w^T T_w - D_w^T (T_P - T_W) \tag{3.12}$$

For further derivation, we should discretize the total flux terms. We consider three different schemes, regarding the discretization of the total flux. Now, we shall examine these schemes respectively.

3.2.1 Central Difference Scheme to Discretize the Conservation of Energy Equation

We apply the linear variation approach to our dependent variable T_e as follows:

$$F_e^T T_e = \frac{F_e^T}{2}(T_P + T_E) \tag{3.13}$$

where, the factor ½ arises from the assumption of the interfaces being midway; some other interpolation factors would have appeared for differently located interfaces. Therefore, the total flux term at *e*-interface leads to

$$J_e^T = \frac{F_e^T}{2}(T_P + T_E) - D_e^T (T_E - T_P) \tag{3.14}$$

Using the expression of

$$F_e^T = \left|F_e^T\right| - 2[\![-F_e^T , 0]\!] \tag{3.15}$$

and rearranging the terms, we obtain

$$J_e^T = F_e^T T_P + [\![F_e^T, 0]\!] (T_E - T_P) + D_e^T \left(1 - \frac{|F_e^T|}{2D_e^T} \right) (T_E - T_P) \tag{3.16}$$

In a similar manner, we obtain the total flux at interface w as:

$$J_w^T = F_w^T T_P + [\![F_w^T, 0]\!] (T_W - T_P) + D_w^T \left(1 - \frac{|F_w^T|}{2D_w^T} \right) (T_W - T_P) \tag{3.17}$$

If we substitute Eqs. (3.16) and (3.17) into Eq. (3.7), we obtain

$$\frac{\rho_P^0 (\Delta z)_P (A_x)_P}{\Delta t} \left(T - T^0 \right)_P + \left[D_e^T \left(1 - \frac{|F_e^T|}{2D_e^T} \right) + [\![-F_e^T, 0]\!] \right] (T_E - T_P)$$

$$+ \left[D_w^T \left(1 - \frac{|F_w^T|}{2D_w^T} \right) + [\![F_w^T, 0]\!] \right] (T_W - T_P)$$

$$= \left(S_c^T \right)_P (\Delta z)_P (A_x)_P + \left(S_p^T \right)_P T_P (\Delta z)_P (A_x)_P \tag{3.18}$$

Rearranging this final form of the conservation of energy equation for central difference, we obtain

$$a_P^T T_P = a_P^T T_E + a_W^T T_W + b^T \tag{3.19}$$

where

$$a_E^T = D_e^T \left(1 - \frac{|F_e^T|}{2D_e^T} \right) + [\![-F_e^T, 0]\!] \tag{3.20}$$

$$a_W^T = D_w^T \left(1 - \frac{|F_w^T|}{2D_w^T} \right) + [\![F_w^T, 0]\!] \tag{3.21}$$

$$\left(a_P^T \right)^0 = \frac{\rho_P^0 (\Delta z)_P (A_x)_P}{\Delta t} \tag{3.22}$$

$$b^T = \left(S_c^T \right)_P (\Delta z)_P (A_x)_P + \left(a_P^T \right)^0 T_P{}^0 \tag{3.23}$$

$$a_P^T = a_E^T + a_W^T + \left(a_P^T\right)^0 - \left(S_P^T\right)_P (\Delta z)_P (A_x)_P \tag{3.24}$$

3.2.2 Upwind Scheme to Discretize the Conservation of Energy Equation

The upwind scheme recognises a different way for the assumption that the convected property T_e at the interface is the average of T_E and T_P, and proposes a better prescription. According to upwind scheme the value of the dependent variable T in convection term at the interface is equal to the value of T at the grid point on the *upwind* side of the face. Thus,

$$T_e = T_E \qquad if \qquad F_e^T < 0 \tag{3.25}$$

$$T_e = T_P \qquad if \qquad F_e^T > 0 \tag{3.26}$$

Base on this assumption, we can use the formulation given below for the upwind scheme

$$F_e^T T_e = \left[\!\left[F_e^T, 0 \right]\!\right] T_P - \left[\!\left[-F_e^T, 0 \right]\!\right] T_E \tag{3.27}$$

If we substitute this equation into Eq. (3.15), we obtain

$$J_e^T = \left[\!\left[F_e^T, 0 \right]\!\right] T_P - \left[\!\left[-F_e^T, 0 \right]\!\right] T_E - D_e^T (T_E - T_P) \tag{3.28}$$

After rearranging these terms, we obtain

$$J_e^T = F_e^T T_P - \left[\!\left[F_e^T, 0 \right]\!\right] (T_E - T_P) - D_e^T (T_E - T_P) \tag{3.29}$$

The final form of the total flux at the w-interface can easily be obtained by using a similar derivation:

$$J_w^T = F_w^T T_P - \left[\!\left[F_w^T, 0 \right]\!\right] (T_W - T_P) - D_w^T (T_W - T_P) \tag{3.30}$$

Therefore, the coefficients of the neighbour points in Eq. (3.19) are written as

$$a_E^T = D_e^T + [\![-F_e^T, 0]\!] \tag{3.31}$$

$$a_W^T = D_w^T + [\![F_w^T, 0]\!] \tag{3.32}$$

The other coefficients for the *upwind* scheme remain the same as in the central difference scheme.

3.2.3 Hybrid Scheme to Discretize the Conservation of Energy Equation

When the strength of the convection is dominant to the diffusion, the upwind scheme gives better results than central difference, and when the situation is the contrary, the central difference is preferred. Therefore, we have to examine and compare the values of these coefficients before we solve any convection-conduction problem.

The name *hybrid* is the indicative of a combination of the central difference and upwind schemes. Therefore, hybrid scheme applies the upwind method, while

$$|P| > 2 \tag{3.33}$$

It applies central difference method while

$$|P| < 2 \tag{3.34}$$

where P is a Peclet number defined by

$$P \equiv \frac{F^T}{D^T}$$

The automatic selection of scheme is provided by the formulation of the total flux term given below:

$$J_e^T = F_e^T T_P + \left\{ [\![-F_e^T, 0]\!] + D_e^T \left[\!\!\left[1 - \frac{|F_e^T|}{2D_e^T}, 0 \right]\!\!\right] \right\} (T_E - T_P) \tag{3.35}$$

Similarly, we obtain the total flux at the w-interface as

$$J_w^T = F_w^T T_P + \left\{ \left[\!\left[F_w^T , 0 \right]\!\right] + D_w^T \left[\!\left[1 - \frac{\left| F_w^T \right|}{2D_w^T} , 0 \right]\!\right] \right\} (T_W - T_P) \tag{3.36}$$

Using these equations, we can obtain the coefficients of neighbour points as follows

$$a_E^T = \left[\!\left[-F_e^T , 0 \right]\!\right] + D_e^T \left[\!\left[1 - \frac{\left| F_e^T \right|}{2D_e^T} , 0 \right]\!\right] \tag{3.37}$$

$$a_W^T = \left[\!\left[F_w^T , 0 \right]\!\right] + D_w^T \left[\!\left[1 - \frac{\left| F_w^T \right|}{2D_w^T} , 0 \right]\!\right] \tag{3.38}$$

The other coefficients remain the same [such as, Eq (3.22)-(3.24)].

3.3 Discretization Equations for the Momentum Balance Equation

In this section we shall discretize the momentum balance equation [17,18]. Integrating Eq. (2.6) over the cross sectional area perpendicular to z-direction, this equation becomes one dimensional:

$$\frac{\partial(\rho v_z)}{\partial t}A_x + \frac{\partial(\rho v_z v_z)}{\partial z}A_x = -\frac{\partial p_d}{\partial z}A_x + \mu\frac{\partial^2 v_z}{\partial z^2}A_x - \tau \mathrm{P} - \rho g\beta(T - T_0)A_x \tag{3.39}$$

where τ is the shear stress and P is the perimeter. Shear stress can be written as

$$\tau = 0.5\rho v_z |v_z| f \tag{3.40}$$

where f is the friction factor. For laminar flow and round tube, friction factor is given as [12]

$$f = \frac{16}{Re_{D_h}} \tag{3.41}$$

Substitute Eq. (3.41) into Eq. (3.39) to give

$$\frac{\partial(\rho v_z)}{\partial t}A_x + \frac{\partial(\rho v_z v_z)}{\partial z}A_x$$

$$= -\frac{\partial p_d}{\partial z}A_x + \mu\frac{\partial^2 v_z}{\partial z^2}A_x - \frac{1}{2}\rho v_z |v_z| f \mathrm{P} - \rho g\beta(T - T_0)A_x \tag{3.42}$$

A total flux term for momentum balance equation can be defined as

$$J^u = \rho v_z v_z A_x - \mu\frac{\partial v_z}{\partial z}A_x \tag{3.43}$$

Substituting this total flux term into Eq. (3.42) and integrating Eq. (3.42) over the control volume shown in Figure 3.1b, one can obtain

$$\left(\frac{\rho v_z - \rho^0 v_z{}^0}{\Delta t}\right)(\delta z)_e (A_x)_e + J_E^u - J_P^u$$

$$= S_c^u (\delta z)_e (A_x)_e + S_p^u (v_z)_e (A_{surf})_e + (p_{dP} - p_{dE})(A_x)_e \tag{3.44}$$

where,

$$\left(S_c^u\right)_e = \rho g \beta \left(T_e - T_0\right) \tag{3.45}$$

$$\left(S_P^u\right)_e = -\frac{1}{2}\left(\rho \left|v_z\right| f\right)_e \tag{3.46}$$

$$J_E^u = \left(\rho v_z v_z A_x\right)_E - \left(\mu \frac{\partial v_z}{\partial z} A_x\right)_E \tag{3.47}$$

$$J_P^u = \left(\rho v_z v_z A_x\right)_P - \left(\mu \frac{\partial v_z}{\partial z} A_x\right)_P \tag{3.48}$$

It can easily be seen that the form of momentum balance equation given by Eq. (3.44) is very similar to the form of conservation of energy equation given by Eq. (3.7). Therefore, further derivations and discretizations are also similar, and, one can easily obtain the momentum balance equation for the hybrid scheme as follows:

$$a_e^u \left(v_z\right)_e = a_{ee}^u \left(v_z\right)_{ee} + a_w^u \left(v_z\right)_w + b^u + \left(p_P - p_E\right)\left(A_x\right)_e \tag{3.49}$$

where

$$a_{ee}^u = [\![-F_E, 0]\!] + D_E \left[\!\!\left[1 - \frac{1}{2}\left|\frac{F_E}{D_E}\right|, 0 \right]\!\!\right] \tag{3.50}$$

$$a_w^u = [\![F_P, 0]\!] + D_P \left[\!\!\left[1 - \frac{1}{2}\left|\frac{F_P}{D_P}\right|, 0 \right]\!\!\right] \tag{3.51}$$

$$\left(a_e^u\right)^0 = \frac{\left(\rho^0\right)_e (\delta x)_e \left(A_x\right)_e}{\Delta t} \tag{3.52}$$

$$b^u = \left(S_c^u\right)_e (\delta x)_e \left(A_x\right)_e + \left(a_P^u\right)^0 {T_P}^0 \tag{3.53}$$

$$a_e^u = a_{ee}^u + a_w^u + \left(a_e^u\right)^0 - \left(S_P^u A_{surf}\right)_e \tag{3.54}$$

3.4 Derivation of the Pressure Correction Equation

The momentum balance equation can be solved only when the pressure field is given or somehow estimated. An equation for obtaining the pressure field can be derived as follows [17-18]:

The momentum balance equation given by Eq. (3.49) can be rewritten as

$$(v_z)_e = \frac{a_{ee}^u (v_z)_{ee} + a_w^u (v_z)_{ee} + b^u}{a_e^u} + d_e (p_P - p_E) \tag{3.55}$$

where

$$d_e \equiv \frac{(A_x)_e}{a_e^u} \tag{3.56}$$

From now on, a pressure correction equation to give the error on pressure will be derived. The imperfect velocity field based on a guessed pressure field p^* will be denoted by v^*. This starred velocity field will result from the solution of the following discretization equation:

$$a_e^u (v_z^*)_e = a_{ee}^u (v_z^*)_{ee} + a_w^u (v_z^*)_w + b^u + (p_P^* - p_E^*)(A_x)_e \tag{3.57}$$

Our aim is to find a way of improving the guessed pressure p' such that the resulting starred velocity field will progressively get closer to satisfying the continuity equation. Let us propose that the correct pressure p be obtained from

$$p = p^* + p' \tag{3.58}$$

where p' will be called the *pressure correction*. Next, we need to know how the velocity components respond to this change in pressure. The corresponding velocity correction v_z' can be introduced similarly as:

$$v_z = v_z^* + v_z' \tag{3.59}$$

If we subtract equation (3.57) from Eq. (3.49), we obtain

$$a_e^u\left(v_z^{'}\right)_e = a_{ee}^u\left(v_z^{'}\right)_{ee} + a_w^u\left(v_z^{'}\right)_w + b^u + \left(p_P^{'} - p_E^{'}\right)\left(A_x\right)_e \tag{3.60}$$

At this point we shall boldly decide to drop the terms of neighbour points, i.e. $a_{ee}^u\left(v_z^{'}\right)_{ee} + a_w^u\left(v_z^{'}\right)_w$, from Eq. (3.60). The result is

$$a_e^u\left(v_z^{'}\right)_e = \left(p_P^{'} - p_E^{'}\right)\left(A_x\right)_e \tag{3.61}$$

or

$$\left(v_z^{'}\right)_e = d_e\left(p_P^{'} - p_E^{'}\right) \tag{3.62}$$

Equation (3.59) is called the velocity correction formula, which can also be written as

$$\left(v_z\right)_e = \left(v_z^{*}\right)_e + d_e\left(p_P^{'} - p_E^{'}\right) \tag{3.63}$$

Similarly, the velocity correction equation for $\left(v_z\right)_w$ can also be derived.

Thus, we have all the preparation needed for obtaining a discretization equation for $p^{'}$. An equation for the pressure correction can be derived from the one dimensional continuity equation. For the purpose of this derivation, we shall assume that the density ρ does not directly depend on pressure. The one dimensional continuity equation (in z-direction) is

$$\frac{\partial \rho}{\partial t} + \frac{\partial\left(\rho v_z\right)}{\partial z} = 0 \tag{3.64}$$

Employing the fully implicit method, the integration of Eq. (3.64) over the control volume shown in Figure 3.1a gives

$$\frac{\left(\rho - \rho^0\right)_P}{\partial t}\left(\Delta z\right)_P\left(A_x\right)_P + \left[\left(\rho v_z\right)_e - \left(\rho v_z\right)_w\right]\left(A_x\right)_P = 0 \tag{3.65}$$

Let us substitute velocity correction equations, Eq.3.63), into the continuity equation, Eq. (3.65), and rearrange it to obtain the following discretization equation for $p^{'}$:

$$a_P^{p'}\, p'_P = a_E^{p'}\, p'_E + a_W^{p'}\, p'_W + b^{p'} \tag{3.66}$$

where

$$a_E^{p'} = (\rho d A_x)_e \tag{3.67}$$

$$a_W^{p'} = (\rho d A_x)_w \tag{3.68}$$

$$a_P^{p'} = a_E^{p'} + a_W^{p'} \tag{3.69}$$

$$b^{p'} = \frac{(\rho^0 - \rho)_P}{\Delta t}(\Delta z)_P (A_x)_P + \left[(\rho v_z^*)_w - (\rho v_z^*)_e\right](A_x)_P = 0 \tag{3.70}$$

3.5 SIMPLE Algorithm

The procedure that we use for the calculation of the flow field, together with the pressure and temperature fields has been given the name SIMPLE, which stands for Semi-Implicit Method for Pressure-Linked Equation. The important operations for the execution of this algorithm are summarized in the flow chart shown in Fig. 3.2.

3.6 Inflow and Outflow Boundary Conditions for the Subchannel

In this thermal-hydraulic model of I.T.U. TRIGA Mark-II reactor, the following set of boundary conditions is used.

Velocity and temperature are specified at the inflow boundary whereas pressure is specified at the outflow boundary.

On the other hand two different approaches are employed at the boundaries, which are

1) zero control volume at the boundaries for the grid shown in Fig. 3.1a for the conservation of energy, pressure and pressure correction equations and,
2) half control volume at the boundaries for the staggered grid shown in Fig. 3.1b for the momentum balance equation.

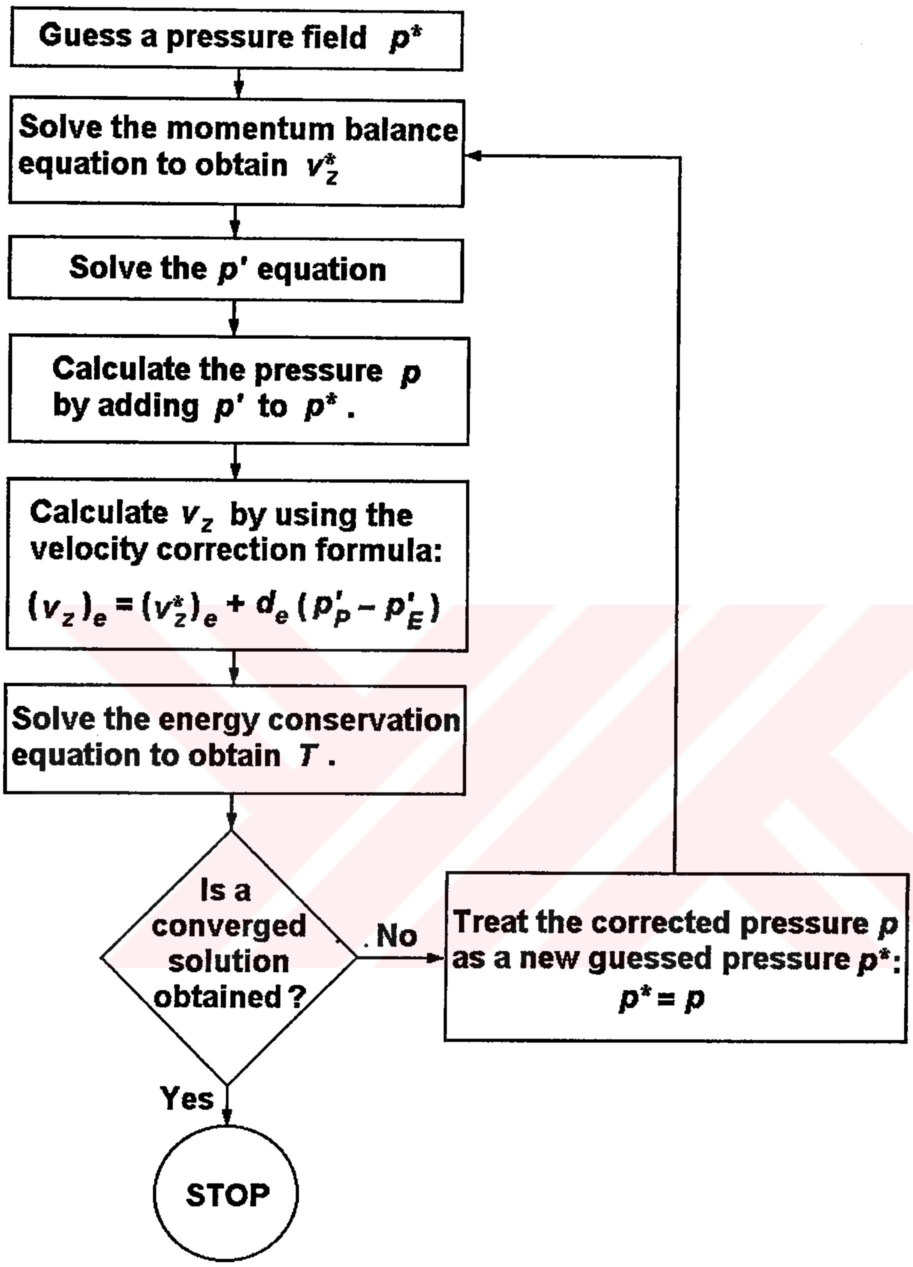

Figure 3.2 The SIMPLE Algorithm

3.7 Solution of the Linear Algebraic Equations

The solution of the discretization equations for the one-dimensional situation can be obtained by the standard Gauss-elimination method, which is sometimes called the Thomas Algorithm or the TDMA (TriDiagonal Matrix Algorithm).

3.8 Heat Conduction Equation for the Fuel Rods

One-dimensional heat conduction equation in cylindrical coordinates is [15]:

$$\frac{\partial(\rho c_v T)}{\partial t} = \frac{1}{r}\frac{\partial}{\partial r}\left(kr\frac{\partial T}{\partial r}\right) + q''' \qquad (3.71)$$

To obtain a discretization equation, the fuel element has been divided to a number of control volumes shown in Figs.3.3 and 3.4. The control volumes take place at the inner and outer material boundaries having imaginary zero width. The control volume # 1 is in the center of the fuel element and the control volume # N is at the outer surface of the clad. A grid point also takes place over the control volume # N. This grid point denotes the coolant [17,18].

In heat conduction equation, heat source term consists of only volumetric heat strength q''' that can be written as:

$$q''' = S^h \qquad (3.72)$$

The heat source S^h can be a constant or any function of temperature. Thus, it can be linearized as

$$S^h = S_c^h + S_P^h T_P \qquad (3.73)$$

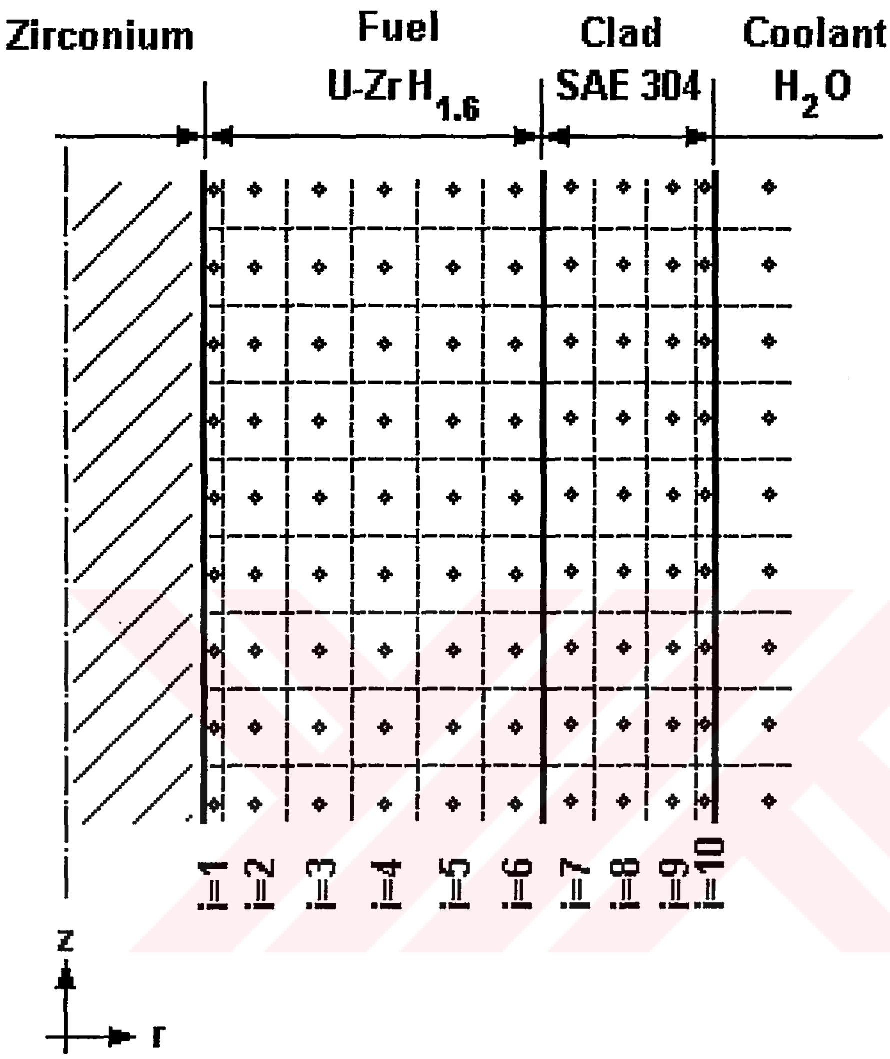

Figure 3.3 Two dimensional grid structure for the fuel rod.

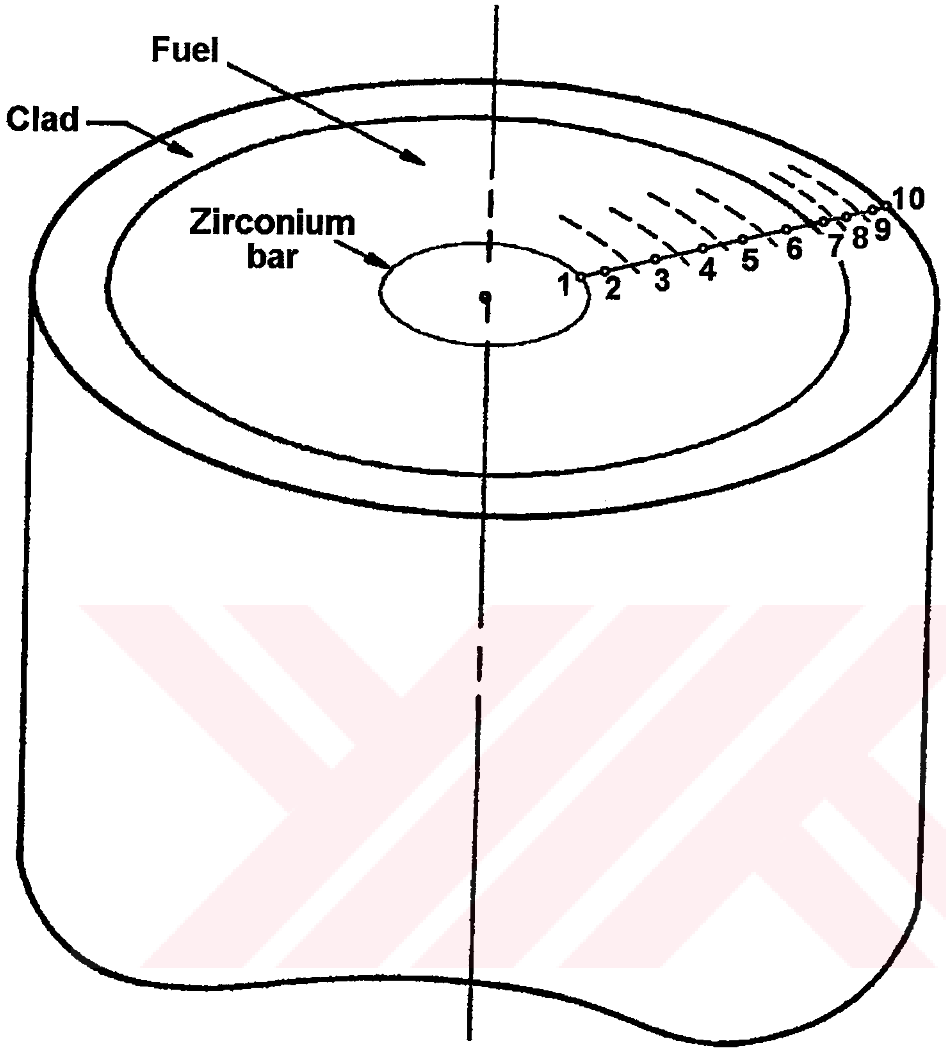

Figure 3.4 Grid for the fuel rod in radial direction.

We assume that density ρ and specific heat c_v are independent from time and displacement. We use average values for these variables. Thus, after rearrangement, Eq. (3.71) becomes:

$$\rho c_v \frac{\partial T}{\partial t} = k\left[\frac{1}{r}\frac{\partial}{\partial r}\left(r\frac{\partial T}{\partial r}\right)\right] + S_c^h + S_P^h T_P \tag{3.74}$$

If we integrate Eq. (3.74) over the control volume shown in Figure 3.2, using fully implicit method, and employ piecewise-linear profile assumption, the resulting equation will be

$$(\rho c_v)_P\left(\frac{r_e + r_w}{2}\right)(\Delta r)_P\left(\frac{T - T^0}{\Delta t}\right)_P = \frac{(r\,k)_e}{(\delta r)_e}(T_E - T_P) - \frac{(r\,k)_w}{(\delta r)_w}(T_P - T_W)$$

$$+\left(S_c^T\right)_P\left(\frac{r_e + r_w}{2}\right)(\Delta r)_P + \left(S_P^T\right)_P\left(\frac{r_e + r_w}{2}\right)(\Delta r)_P\, T_p \tag{3.75}$$

Hence, we have reached the form of the heat conduction equation that can be also written as an equation of coefficients:

$$a_P^T T_P = a_P^T T_E + a_W^T T_W + b^T \tag{3.76}$$

where

$$a_E^T = \frac{r_e\, k_e}{(\delta r)_e} \tag{3.77}$$

$$a_W^T = \frac{r_w\, k_w}{(\delta r)_w} \tag{3.78}$$

$$\left(a_P^T\right)^0 = \frac{(\rho c_v)_P}{\Delta t}\left(\frac{r_e + r_w}{2}\right)(\Delta r)_P \tag{3.79}$$

$$b^T = \left(S_c^T\right)_P\left(\frac{r_e + r_w}{2}\right)(\Delta r)_P + \left(a_P^T\right)^0 T_P{}^0 \tag{3.80}$$

$$a_P^T = a_E^T + a_W^T + \left(a_P^T\right)^0 - \left(S_P^T\right)_P\left(\frac{r_e + r_w}{2}\right)(\Delta r)_P \tag{3.81}$$

3.9 Boundary Conditions For Heat Conduction Problem in the Fuel Rods

The *zero control volume* approach is employed for the boundaries of fuel rods, while solving heat conduction equation for them.

Since fluid flow does not exist in a heat conduction problem, the previous rules for the *outflow* boundaries are not valid here. Thus, we need the boundary conditions for both boundaries in radial direction.

In this application, we have used the $q'' = 0$ *boundary condition* at the interface between the fuel and zirconium rod. Since there is no heat source or sink, the temperature is constant in radial direction in the zirconium rod. At the outer surface of the clad, heat flux is specified via a heat transfer coefficient and the temperature of the surrounding fluid, where heat flux is calculated using Eq. (3.82). The value of heat flux between the clad surface and the coolant is obtained by an iterative solution procedure of the set of algebraic equations.

$$q'' = hA_{surf}\left(T_{cl} - T_m\right) \tag{3.82}$$

where T_{cl} and T_m are the clad outer surface and coolant temperatures.

CHAPTER 4

RESULTS AND CONCLUSIONS

4.1 Computational Results

After the completion of the development of a FORTRAN program which employs SIMPLE algorithm to solve the set of algebraic equations, it was run to obtain some temperature, pressure and velocity distributions for the coolant together with the temperature distribution through fuel rods of I.T.U. TRIGA Mark-II reactor.

Some of the geometrical dimensions used in the thermal-hydraulic model in the sample runs of this computer code are given in Table 4.1.

Table 4.1 Dimensions of the fuel rods of I.T.U. TRIGA Mark-II reactor [1,2].

	RADIUS
Radius of zirconium filling material	0,3175 cm
Radial position of thermocouple	0,762 cm
Fuel outer radius	1,8161 cm
Clad outer radius	1,8669 cm

In the sample runs of the computer code developed by this study, the used fuel element thermal power values of different fuel rods that correspond to a maximum steady reactor power of 250 kW of I.T.U. TRIGA Mark-II reactor are summarized in Table 4.2. A cosine linear power density variation is considered in all runs of the computer code.

Table 4.2 Calculated thermal power values of different fuel rods of I.T.U. TRIGA Mark-II reactor that correspond to a maximum steady reactor power of 250 kW.

POSITION	P_{max} (w)
B1	5364
C1	4756
D1	3888
E1	2984
F1	2564

Grid structure in radial direction and some thermophysical properties of fuel element B1 of I.T.U. TRIGA Mark-II reactor are also summarized in Table 4.3. It can be seen from Table 4.3 that specific heat at constant pressure of fuel and conductivities of fuel and clad are temperature dependent and calculated by the aid of the correlations given in literature [5].

Table 4.3 Grid structure in radial direction and some thermophysical properties of fuel element B1 of I.T.U. TRIGA Mark-II reactor [5].

r_{in} (cm)	r_{out} (cm)	k (W/m-K)	c_p (kj/kg-K)	ρ (kg/m^3)
0,3175	0,3175	18,71	1048,33	6000
0,3175	0,3275	18,71	1048,33	6000
0,3275	0,6232	18,71	1048,22	6000
0,6232	0,9189	18,68	1043,18	6000
0,9189	1,2147	18,64	1034,32	6000
1,2147	1,5104	18,57	1021,90	6000
1,5104	1,8061	18,49	1006,00	6000
1,8061	1,8161	18,44	996,01	6000
1,8161	1,8324	15,09	460,00	7865
1,8324	1,8486	15,08	460,00	7865
1,8486	1,8649	15,06	460,00	7865
1,8649	1,8669	15,06	460,00	7865
1,8669	1,8669	15,06	460,00	7865

Grid structure in axial direction and some thermophysical parameters of coolant used in the thermal-hydraulic model of I.T.U. TRIGA Mark-II reactor are also presented in Table 4.4 that are calculated by the aid of the program H2O [3].

Table 4.4 Grid structure in axial direction and some thermophysical parameters of coolant in subchannel B1 used in the thermal-hydraulic model of I.T.U. TRIGA Mark-II reactor [3].

z_{in} (cm)	z_{out} (cm)	k (W/m-K)	c_p (kj/kg-K)	ρ (kg/m^3)	h (W/m-K)	β (1/K)	μ (kg/m-s)
-19,05	-16,51	0,628	4178,86	994,80	1106,25	0.00035	0,00075
-16,51	-13,97	0,629	4178,38	994,56	1161,85	0.00035	0,00074
-13,97	-11,43	0,630	4177,83	994,27	1206,22	0.00035	0,00072
-11,43	-8,89	0,631	4177,23	993,94	1242,09	0.00035	0,00071
-8,89	-6,35	0,633	4176,62	993,56	1270,87	0.00035	0,00070
-6,35	-3,81	0,634	4176,00	993,16	1293,29	0.00035	0,00068
-3,81	-1,27	0,636	4175,41	992,73	1309,66	0.00035	0,00067
-1,27	1,27	0,637	4174,85	992,28	1320,03	0.00035	0,00065
1,27	3,81	0,639	4174,34	991,83	1324,21	0.00035	0,00064
3,81	6,35	0,640	4173,89	991,39	1321,86	0.00035	0,00063
6,35	8,89	0,641	4173,50	990,96	1312,43	0.00035	0,00061
8,89	11,43	0,642	4173,17	990,56	1295,11	0.00035	0,00060
11,43	13,97	0,643	4172,91	990,20	1268,70	0.00035	0,00059
13,97	16,51	0,644	4172,71	989,90	1231,33	0.00035	0,00059
16,51	19,05	0,645	4172,55	989,65	1179,79	0.00035	0,00058

Variation of the axial directional coolant velocity and temperature distributions in time for transient regime for subchannel B1 are given in Figures 4.1 and 4.2.

In obtaining the results plotted in Figures 4.1 and 4.2, coolant temperature and velocity are assumed 32.5 ^{o}C and 0.1201 m/s at every position in Subchannel B1 respectively as the initial condition.

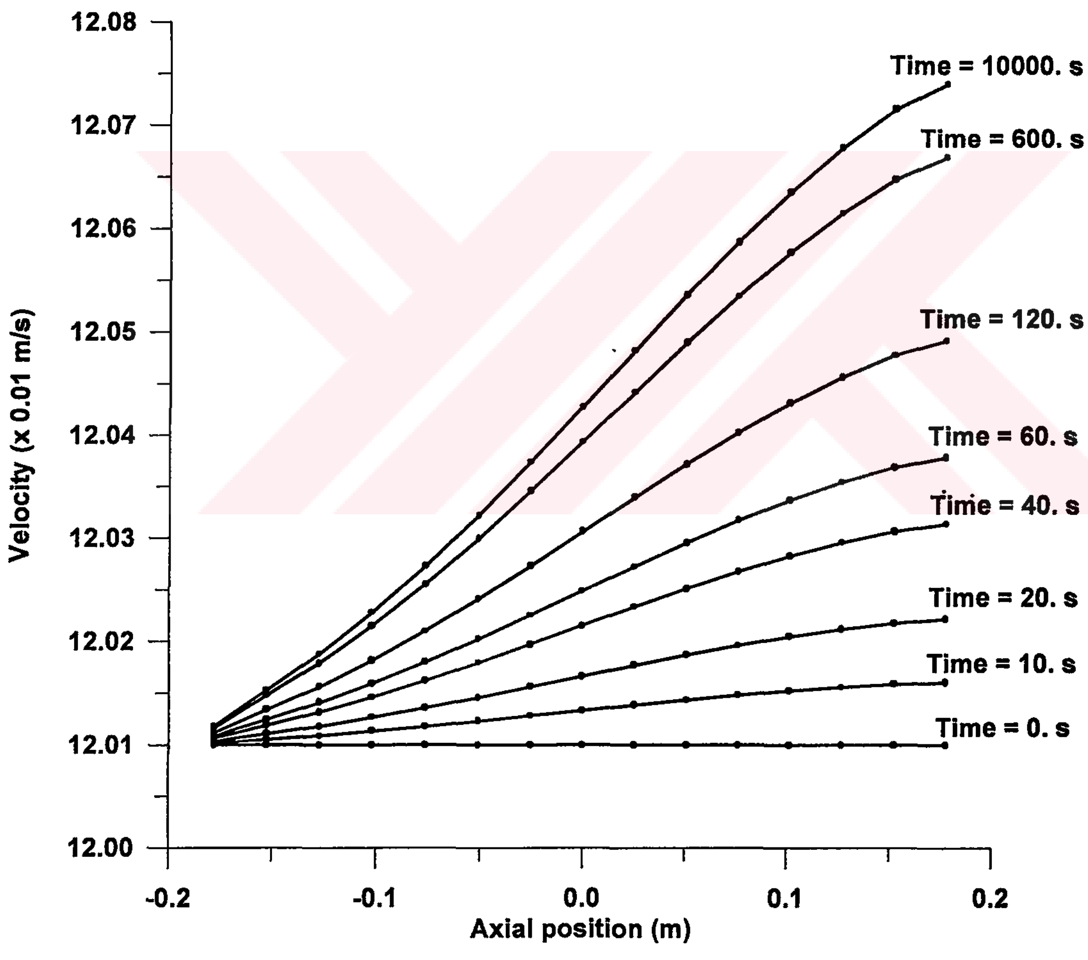

Figure 4.1 Variation of the axial directional coolant velocity distribution in time for subchannel B1

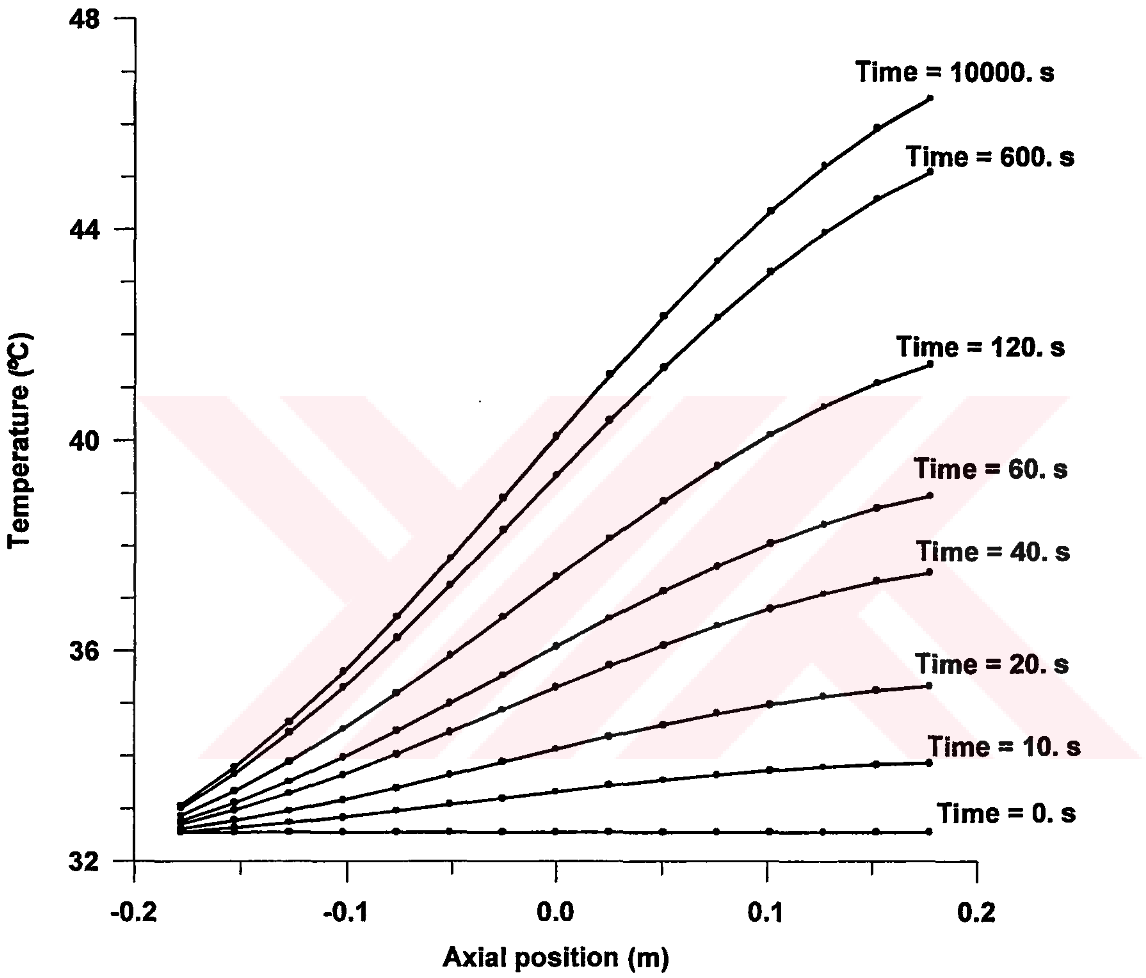

Figure 4.2 Variation of the axial directional coolant temperature distribution in time for subchannel B1

Variations of the axial directional hydraustatic pressure drop and absolute pressure in coolant for subchannel B1 are plotted in Figures 4.3 and 4.4 for steady state regime.

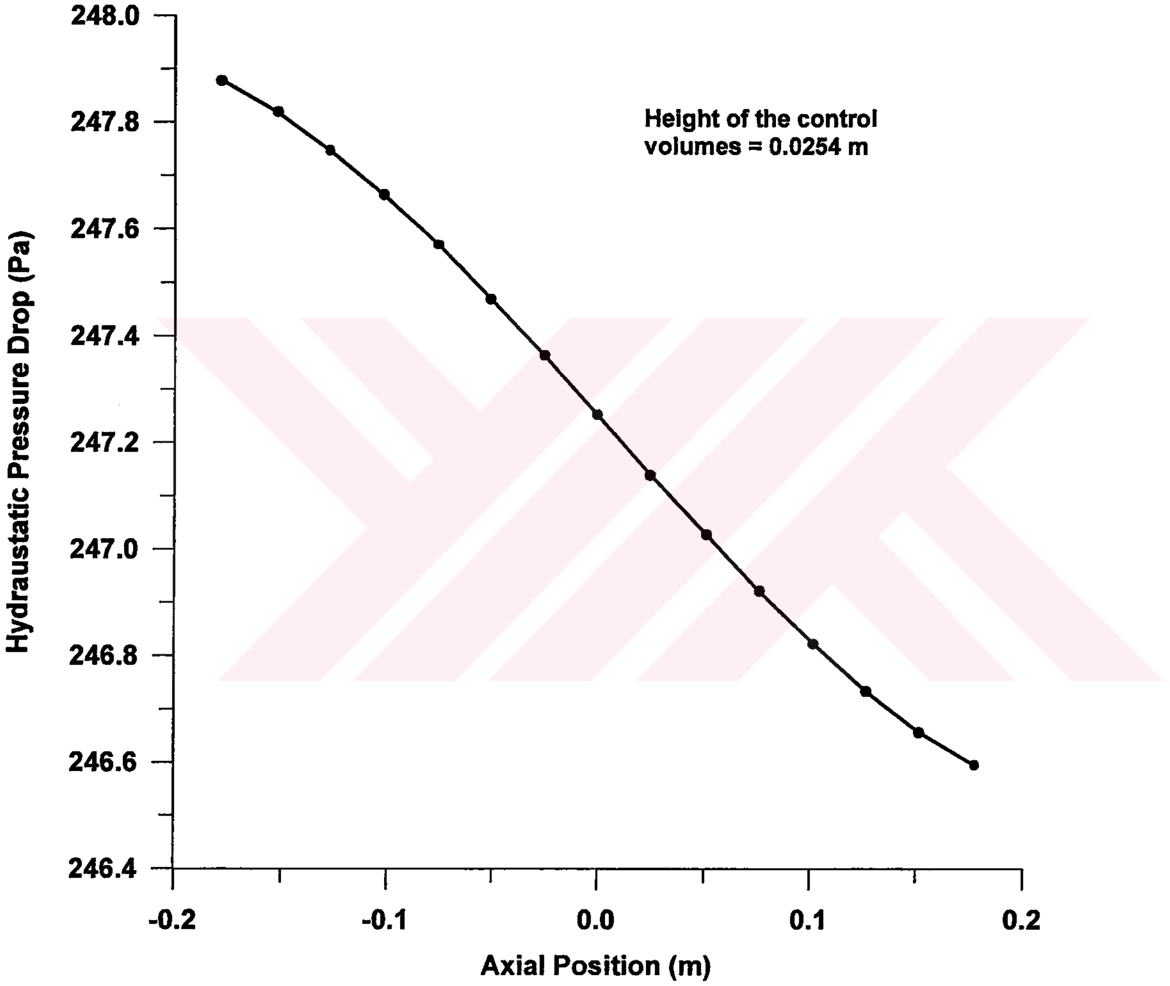

Figure 4.3 Variation of the axial directional hydraustatic pressure drop in coolant for subchannel B1

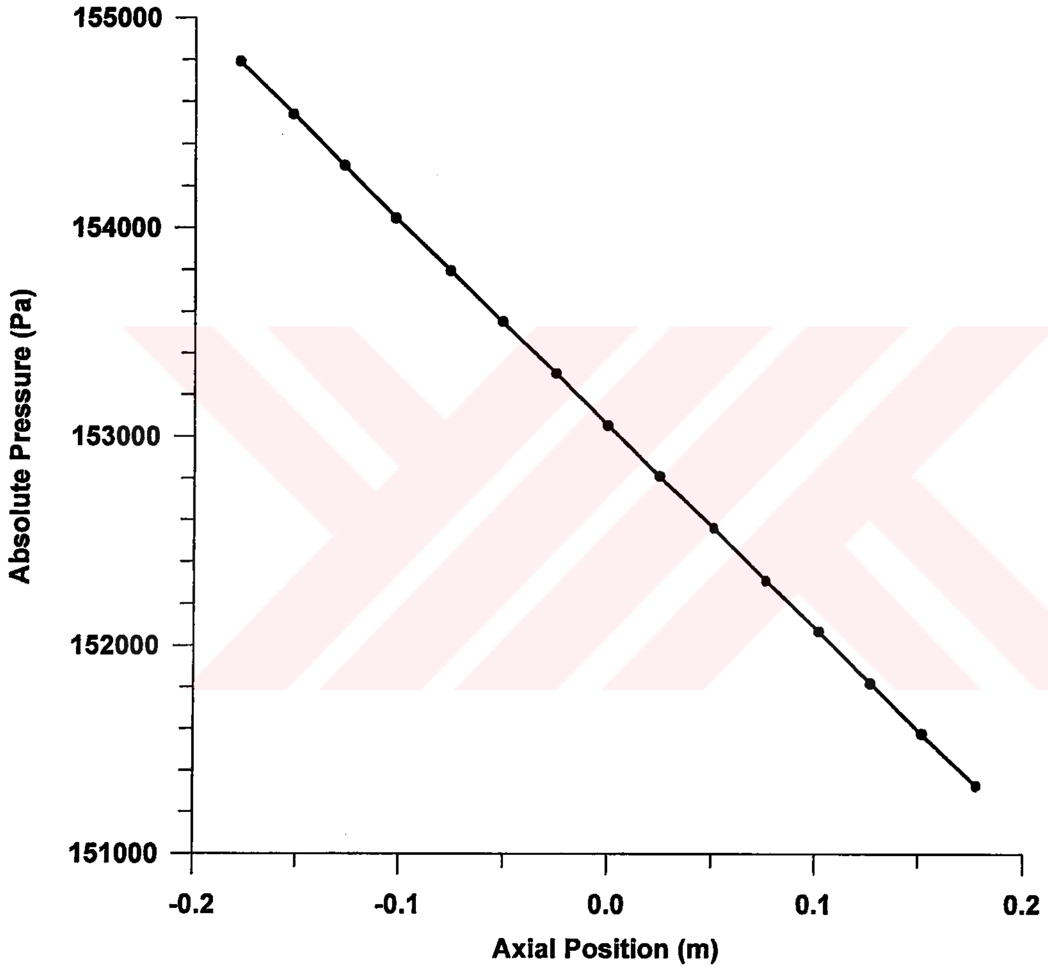

Figure 4.4 Axial directional variation of absolute pressure of coolant for subchannel B1

Variations of the steady state axial directional temperature distribution at different positions of the fuel rod in subchannel B1are plotted in Figures 4.5.

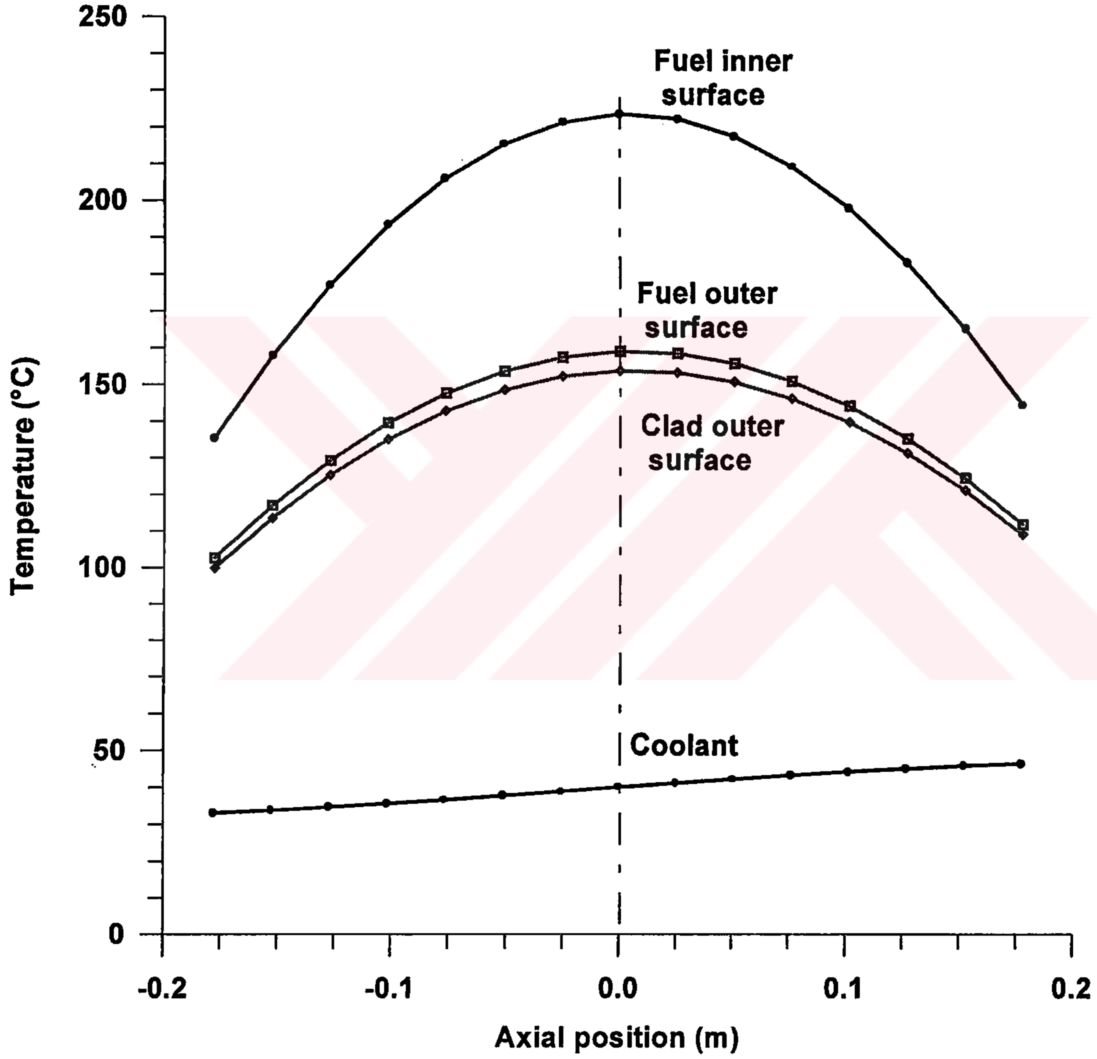

Figure 4.5 Variation of the steady state axial directional temperature distribution at the different positions of the fuel rod for subchannel B1

Variations of the steady state axial fuel temperature distributions at the fuel rod center in different rings plotted in Figures 4.6

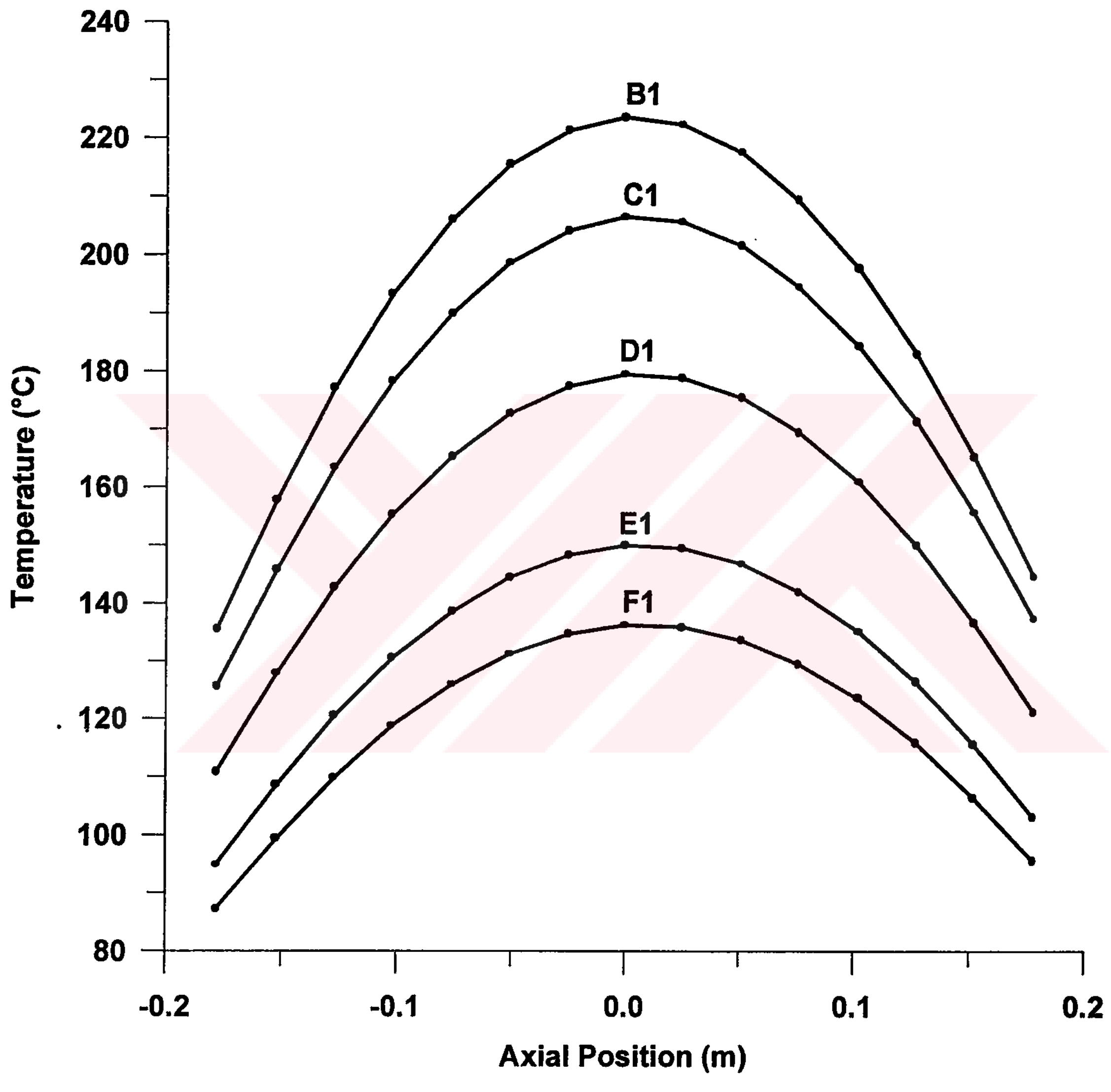

Figure 4.6 Variations of the steady state axial fuel temperature distributions at the fuel rod center in different rings

Variations of the steady state radial temperature distribution in the fuel rods of different rings plotted in Figures 4.7

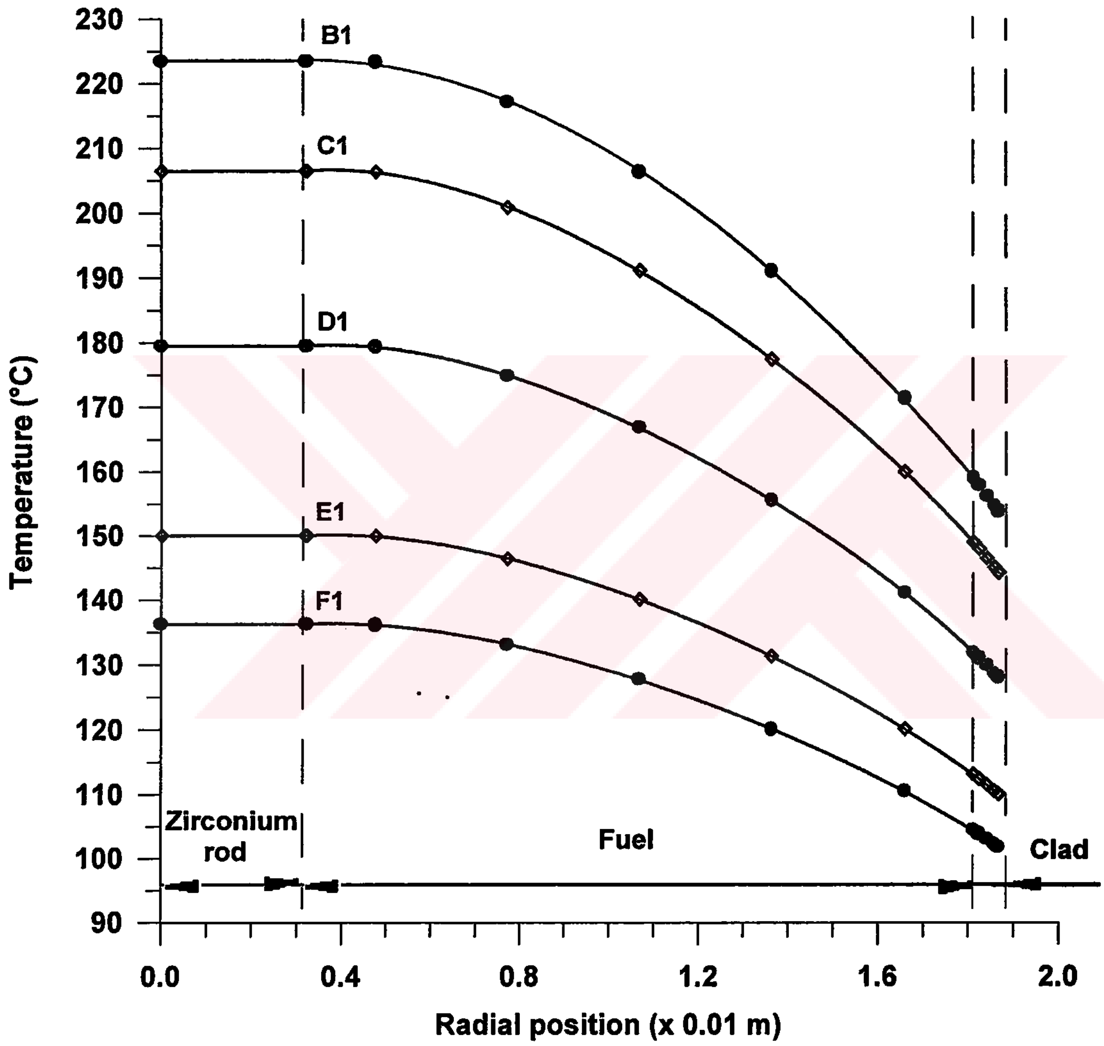

Figure 4.7 Variation of the steady state radial temperature distribution in the fuel rods of different rings

Variation of the steady state radial temperature distribution in fuel rod B1 for different thermal conductivity values of fuel meat are also estimated parametrically and then plotted in Figure 4.8.

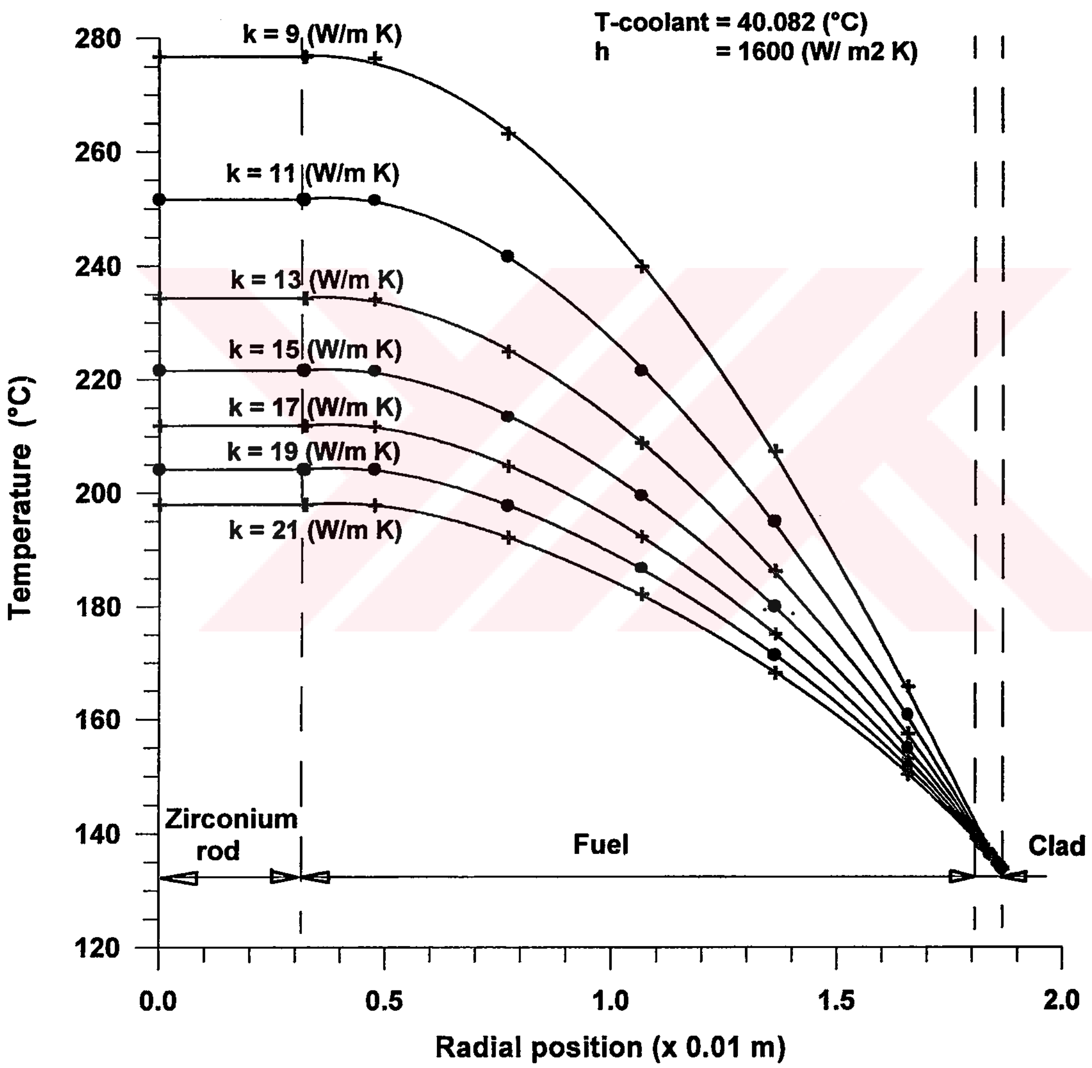

Figure 4.8 Variation of the steady state radial temperature distribution in fuel rod B1 for different thermal conductivity values of fuel meat

Variation of the steady state radial temperature distribution in fuel rod B1 for different convection heat transfer coefficient values are also estimated parametrically and then plotted in Figure 4.9.

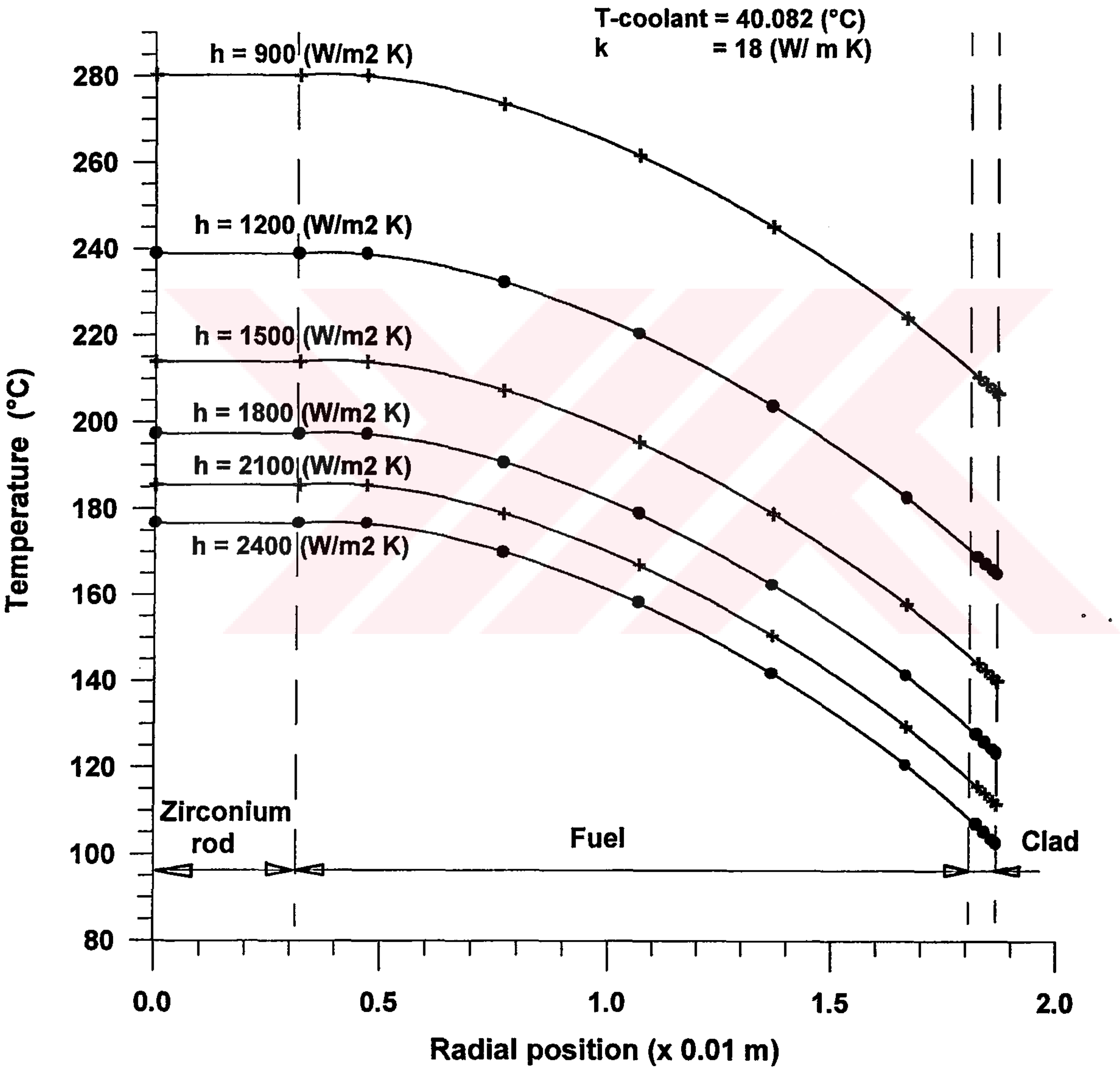

Figure 4.9 Variation of the steady state radial temperature distribution in fuel rod B1 for different convection heat transfer coefficient values

Some dimensionless coefficients of coolant estimated by this study for different control volumes in axial direction in subchannel B1 of I.T.U. TRIGA Mark-II reactor are also summarized in Table 4.5.

Table 4.5 Some dimensionless coefficients of coolant estimated by this study for different control volumes in axial direction in subchannel B1 of I.T.U. TRIGA Mark-II reactor.

z_{in} (cm)	z_{out} (cm)	Re -	Gr ($x10^6$)	Pr -	Ra ($x10^6$)
-19,05	-16,51	4996	6,65	4,98	33,1
-16,51	-13,97	5070	8,17	4,90	40,0
-13,97	-11,43	5158	9,60	4,81	46,1
-11,43	-8,89	5257	10,94	4,70	51,5
-8,89	-6,35	5367	12,16	4,60	55,9
-6,35	-3,81	5484	13,23	4,49	59,4
-3,81	-1,27	5607	14,13	4,38	61,9
-1,27	1,27	5732	14,81	4,27	63,3
1,27	3,81	5856	15,22	4,17	63,5
3,81	6,35	5977	15,32	4,08	62,5
6,35	8,89	6092	15,09	3,99	60,2
8,89	11,43	6198	14,48	3,92	56,7
11,43	13,97	6292	13,47	3,85	51,9
13,97	16,51	6372	12,06	3,80	45,8
16,51	19,05	6436	10,24	3,76	38,5

Axial directional variation of some thermal-hydraulic parameters in subchannel B1 for I.T.U. TRIGA Mark-II reactor are also presented in Table 4.6.

Table 4.6 Axial directional variation of some thermal-hydraulic parameters in subchannel B1 for I.T.U. TRIGA Mark-II reactor

z_{in} (cm)	z_{out} (cm)	V_{fluid} (m/s)	T_{fluid} (°C)	$T_{rod\ centre}$ (°C)	$T_{fuel\ outer}$ (°C)	T_{clad} (°C)
-19,05	-16,51	12,012	33,07	135,47	102,64	99,88
-16,51	-13,97	12,015	33,79	157,82	116,97	113,57
-13,97	-11,43	12,019	34,64	177,13	129,27	125,30
-11,43	-8,89	12,023	35,60	193,25	139,51	135,07
-8,89	-6,35	12,027	36,65	206,05	147,63	142,83
-6,35	-3,81	12,032	37,76	215,41	153,60	148,53
-3,81	-1,27	12,037	38,92	221,26	157,40	152,17
-1,27	1,27	12,043	40,08	223,55	159,02	153,74
1,27	3,81	12,048	41,24	222,29	158,47	153,25
3,81	6,35	12,054	42,35	217,53	155,78	150,72
6,35	8,89	12,059	43,40	209,33	151,00	146,21
8,89	11,43	12,064	44,36	197,80	144,17	139,75
11,43	13,97	12,068	45,21	183,07	135,35	131,40
13,97	16,51	12,072	45,93	165,29	124,58	121,20
16,51	19,05	12,074	46,50	144,58	111,88	109,15

Axial directional variation of the absolute pressure and the pressure components that contribute to the absolute pressure of coolant in subchannel B1 for I.T.U. TRIGA Mark-II reactor are given in Table 4.7. Sum of the columns 4-6 of Table 4.7 gives us the absolute pressure given in column 3 with an imbalance (error) given in the last column. Therefore, this table gives us an idea of the order of errors of this study.

Table 4.7 Axial directional variation of the absolute pressure and the pressure components that contribute to the absolute pressure of coolant in subchannel B1 for I.T.U. TRIGA Mark-II reactor

z_{in} (cm)	z_{out} (cm)	Absolute pressure (Pa)	Dynamic pressure (Pa)	Hydraustatic pressure (Pa)	Atmospheric pressure (Pa)	Pressure imbalance (Pa)
-19,05	-16,51	154789,93	-8,48	53472,80	101325,00	0,61
-16,51	-13,97	154541,99	-8,50	53224,88	101325,00	0,61
-13,97	-11,43	154294,12	-8,44	52976,95	101325,00	0,61
-11,43	-8,89	154046,33	-8,30	52729,03	101325,00	0,60
-8,89	-6,35	153798,63	-8,07	52481,10	101325,00	0,60
-6,35	-3,81	153551,02	-7,75	52233,18	101325,00	0,60
-3,81	-1,27	153303,51	-7,33	51985,25	101325,00	0,60
-1,27	1,27	153056,11	-6,81	51737,33	101325,00	0,59
1,27	3,81	152808,80	-6,19	51489,40	101325,00	0,59
3,81	6,35	152561,60	-5,46	51241,48	101325,00	0,59
6,35	8,89	152314,49	-4,64	50993,55	101325,00	0,58
8,89	11,43	152067,47	-3,73	50745,62	101325,00	0,58
11,43	13,97	151820,53	-2,75	50497,70	101325,00	0,58
13,97	16,51	151573,66	-1,69	50249,77	101325,00	0,58
16,51	19,05	151326,85	-0,57	50001,85	101325,00	0,57

Axial directional variation of different pressure terms that contribute to the momentum balance equation in subchannel B1 for I.T.U. TRIGA Mark-II reactor are also summarized in Table 4.8. The aim of this table is to give an idea about the contributions of all pressure terms and the imbalance in momentum balance equation.

Table 4.8 Axial directional variation of different pressure terms that contribute to the momentum balance equation in subchannel B1 for I.T.U. TRIGA Mark-II reactor

z_{in} (cm)	z_{out} (cm)	Storage (Pa)	Accelarational pressure drop (Pa)	Dynamic pressure difference (Pa)	Frictional pressure drop (Pa)	Diffusion term (Pa)	Buoyancy term (Pa)	Imbalance (Pa)
-19,05	-17,78	0,0000	-0,0027	0,0000	0,0000	0,0000	0,0000	0,0027
-17,78	-15,24	0,0000	0,0048	0,0119	-0,0885	0,0000	0,0810	-0,0004
-15,24	-12,70	0,0000	0,0041	-0,0582	-0,0871	0,0000	0,1491	-0,0003
-12,70	-10,16	0,0000	0,0048	-0,1375	-0,0856	0,0000	0,2276	-0,0003
-10,16	-7,62	0,0000	0,0053	-0,2257	-0,0839	0,0000	0,3147	-0,0002
-7,62	-5,08	0,0000	0,0058	-0,3206	-0,0822	0,0000	0,4085	-0,0002
-5,08	-2,54	0,0000	0,0062	-0,4203	-0,0804	0,0000	0,5067	-0,0001
-2,54	0,00	0,0000	0,0064	-0,5223	-0,0787	0,0000	0,6073	0,0000
0,00	2,54	0,0000	0,0065	-0,6244	-0,0771	0,0000	0,7080	0,0000
2,54	5,08	0,0000	0,0064	-0,7243	-0,0755	0,0000	0,8063	0,0001
5,08	7,62	0,0000	0,0061	-0,8197	-0,0741	0,0000	0,9001	0,0002
7,62	10,16	0,0000	0,0057	-0,9085	-0,0728	0,0000	0,9873	0,0003
10,16	12,70	0,0000	0,0051	-0,9887	-0,0716	0,0000	1,0659	0,0004
12,70	15,24	0,0000	0,0044	-1,0585	-0,0707	0,0000	1,1340	0,0004
15,24	17,78	0,0000	0,0022	-1,1163	-0,0699	0,0000	1,1902	0,0018
17,78	19,05	0,0000	0,0018	-0,5710	-0,0348	0,0000	0,6076	0,0000

The data for the coolant of I.T.U. TRIGA Mark-II reactor obtained from the run of TRISTAN [19] are presented in Table 4.9 in order to make possible a comparison between the results of this study and TRISTAN.

Table 4.9 Some of the thermal-hydraulic parameters obtained from the run of TRISTAN for the coolant of I.T.U. TRIGA Mark-II reactor [19].

Zone	Height (cm)	$T_{average}$ (°C)	Pressure drops (Pa)	Density (g/cm3)	Velocity (cm/s)
15	52,36	46,43	245,73	0,9886	12,07
14	49,82	45,76	245,57	0,9899	12,07
13	47,28	44,95	245,49	0,9902	12,06
12	44,74	44,01	245,13	0,9906	12,06
11	42,20	42,97	245,22	0,9910	12,05
10	39,66	41,84	245,38	0,9914	12,05
9	37,12	40,67	245,59	0,9919	12,04
8	34,58	39,47	245,84	0,9923	12,04
7	32,04	38,26	246,12	0,9928	12,03
6	29,50	37,09	246,40	0,9932	12,03
5	26,96	35,97	246,69	0,9937	12,02
4	24,42	34,92	247,31	0,9940	12,02
3	21,88	33,98	247,64	0,9944	12,01
2	19,33	33,17	247,87	0,9947	12,01
1	16,80	32,50	248,07	0,9950	12,01

The data which is the estimations for maximum temperatures in the center of fuel, and at the outer surface of fuel and clad in radial direction obtained from the run of TRISTAN for I.T.U. TRIGA Mark-II reactor is also given in Table 4.10 to make a comparison [19].

Table 4.10 Maximum temperatures obtained from the run of TRISTAN for the fuel rods in different rings of I.T.U. TRIGA Mark-II reactor [19].

POSITION	T_{max} (°C)	T_f (°C)	T_C (°C)
B1	256	141	133
C1	230	134	126
D1	213	127	123
E1	183	118	113
F1	147	91	88

The data given in Table 4.11 is the result of measurements for the maximum temperatures in the center of fuels at different rings of I.T.U. TRIGA Mark-II reactor [19]. It is also given for comparison.

Table 4.11 Experimentally obtained maximum temperatures in different fuel rods of I.T.U. TRIGA Mark-II reactor [19].

POSITION	T (°C)
B1	244
C1	219
D1	204
E1	176
F1	141

4.2 Conclusions

In this study, a transient, one-dimensional thermal-hydraulic subchannel analysis for ITU TRIGA Mark-II reactor was employed. Mixed convection is considered in modelling to enhance the capability of the computer code. After the continuity, conservation of energy, momentum balance equations for coolant in axial direction and heat conduction equation for fuel rod in radial direction had been written, they were discretized by using the control volume approach to obtain a set of algebraic equations. By the aid of discretized continuity and momentum balance equations, a pressure correction equation was derived. Then, a FORTRAN program has been developed to solve this set of algebraic equations by using SIMPLE algorithm. As a result, the temperature distributions of the coolant and fuel rods as well as the velocity and pressure distributions of the coolant have been estimated for both transient and steady state regimes.

In the evaluation of this study, it is noted that the maximum temperature in the fuel rod is highly dependent on conductivity of fuel which can also be considered either a constant or temperature dependent in different studies given in literature [4-8, 19,20]. A parametric analysis is carried out during this study to determine the conductivity range from the maximum temperature of fuel estimated by this study and the measured temperatures. By the aid of Figure 4.8 and Table 4.11, it can be said that the fuel conductivity must be about 12 W/m K if the convective heat transfer coefficient is considered as 1600 W/m^2 K. Similarly, a parametric analysis is also carried out during this study to determine the effect of convective heat transfer coefficient at the outer surface of cladding on the radial temperature distribution in fuel rod and, thus, on the temperature at the outer surface of cladding.

The data used in the computer code developed by this thesis are mostly the same as those of the TRISTAN. However, some thermal-hydraulic considerations are different between these two codes. As an example, the subchannel is a triangular one in TRISTAN whereas in our study it is a rod centered subchannel. Therefore, hydraulic diameters etc. are also different. Pressure distributions and drops are very close to each other. The convergence of the code of this study is perfect as well as the velocity, and temperature gradients are in good agreement with the results of TRISTAN.

REFERENCES

[1] Safety Analysis Report for the TRIGA Mark-II Reactor for the Institute for Nuclear Energy, Technical University of Istanbul, Turkey, 1978.

[2] TRIGA Mark-II Reactor Mechanical Operation and Maintenance Manual, GA Project 2129, March 1, 1978.

[3] H2O, Calculation of Thermodynamic Properties of Steam and H2O, OECD Nuclear Energy Agency Databank, NEA 0876 0984.

[4] CAN, B., YAVUZ, H., İ.T.Ü. TRIGA Mark-II Reaktörünün Nonlineer Simülasyonu, Yöneylem Araştırması ve Endüstri Mühendisliği 91. Ulusal Kongresi, İ.T.Ü. İstanbul, 17-19 Haziran 1991.

[5] CAN, B., YAVUZ, H., AKBAY, E., The Investigation of Nonlinear Dynamics Behaviour of ITU TRIGA Mark-II Reactor, Eleventh European TRIGA Users Conference, Heidelberg, Germany, 2.39-2.49 Sep.11-13, 1990.

[6] CAN, B., YAVUZ, H., İ.T.Ü. TRIGA Mark-II Reaktörü Termo-Hidrolik Analizi, Marmara Üniversitesi Fen Bilimleri Dergisi, Sayı 2, Say.229-237, İstanbul, 1985.

[7] CAN, B., KURUL, N., BÜKE, T., YAVUZ, H., İ.T.Ü. TRIGA Mark-II Reaktörünün Dinamik Davranışı, 5. Ulusal Nükleer Bilimler Kongresi, Dokuz Eylül Üniversitesi Nükleer Bilimler Enstitüsü İzmir, 22-24 Mayıs 1991.

[8] DASARI, V.R., EL-GENK, M.S., RUBIO, R.A., BRYSON, J.W. FOUSHEE, F.C., Thermal Hydraulics for Sandia's Annular Core Research Reactor, Eleventh Biennial U.S. TRIGA Users' Conference, Washington, D.C., USA, April 10-13, 1988.

[9] TODREAS, N.E., KAZIMI, M.S., Nuclear Systems II, Elements of Thermal Hydraulic Design, Hemisphere Publishing Corp., 1990.

[10] TODREAS, N.E., KAZIMI, M.S., Nuclear Systems I, Thermal Hydraulic Fundamentals, Hemisphere Publishing Corp., 1990.

[11] LAHEY, Jr., R.T. and MOODY, F.J., The Thermal-Hydraulics of a Boiling Water Nuclear Reactor, American Nuclear Society, 1977.

[12] BEJAN, A, Convection Heat Transfer, John Wiley and Sons, 1984.

[13] ARPACI, V., LARSEN, P.S., Convection Heat Transfer, Prentice-Hall Inc., 1984.

[14] WALLIS, G.B., One-Dimensional Two-Phase Flow, Mc Graw-Hill Book Company, 1969.

[15] HOLMAN, J.P., Heat Transfer, McGraw-Hill Book Company, 1989.

[16] SERTELLER, G., Nükleer Yakıt Soğutucu Kanallarında Birleşik Taşınımla Isı Transferinin Sayısal Çözümü, Yüksek Lisans Tezi, İ.T.Ü. Nükleer Enerji Enstitüsü, 1997.

[17] PATANKAR, S.V., Numerical Heat Transfer and Fluid Flow, Hemisphere Publishing Corporation, 1980.

[18] PATANKAR, S.V., SPALDING, D.B., A Calculation Procedure for Heat, Mass and Momentum Transfer in Three-Dimensional Parabolic Flows, Int. J. of Heat and Mass Transfer, Vol. 15, pp.1787-1806, 1972.

[19] BÜKE, T., YAVUZ, H., Calculation of the Flow Parameters in TRIGA Core Coolant Channel, 16th European TRIGA Conference, Pitesti, Romania, 22-25 Sep. 2000, (Accepted for a presentation).

[20] MELE, I., ZEFRAN, B., TRISTAN: A Computer Program for Calculating Natural Convection Flow Parameters in TRIGA Core, University of Ljubljana, Slovenia, 1992.

CURRICULUM VITAE

Emin Hakan ÖZKUL was born as the second child of Emin Aydın and Serpil ÖZKUL in Ankara, Türkiye on June 16, 1975.

He graduated from the Mechanical Engineering Department of Osmangazi University, Eskişehir, Türkiye in August 1998.

He began to work for the study presented in this M. Sc. thesis in the Institute for Nuclear Energy of Istanbul Technical University in September 1999.